

FACILITY FORM 902

N69-24893

(ACCESSION NUMBER)

(THRU)

78

(PAGES)

1

(CODE)

CR# 100892

(NASA CR OR TMX OR AD NUMBER)

30

(CATEGORY)

**JET PROPULSION LABORATORY
CALIFORNIA INSTITUTE OF TECHNOLOGY
PASADENA, CALIFORNIA**

RE-ORDER NO. 68-593

09349-6001-R000

TECHNICAL REPORT

MARS SURFACE SOIL
EROSION STUDY

CONTRACT NO. AX 422060

FEBRUARY 28, 1968

Prepared By

Robert E. Hutton

for

JET PROPULSION LABORATORY
CALIFORNIA INSTITUTE OF TECHNOLOGY
Pasadena, California

This work was performed for the Jet Propulsion Laboratory,
California Institute of Technology, sponsored by the
National Aeronautics and Space Administration under
Contract NAS7-100.

TRW SYSTEMS

ONE SPACE PARK • REDONDO BEACH, CALIFORNIA

ACKNOWLEDGMENTS

The author wishes to express his appreciation to F. C. Vote and J. R. Wrobel of Jet Propulsion Laboratories for the helpful technical discussions during the performance of this study.

CONTENTS

| | Page |
|---------------------------------------|------|
| 1. SUMMARY | 1 |
| 2. INTRODUCTION | 3 |
| 3. RESULTS | 5 |
| 3.1 Surface Loadings | 6 |
| 3.2 Soil Erosion | 16 |
| 3.3 Soil Particle Displacements | 22 |
| 4. REFERENCES | R-1 |

APPENDICES

| | | |
|---|---|------|
| A | ROBERTS' THEORY | A-1 |
| | 1. Definition of Symbols | A-3 |
| | 2. Governing Equations | A-5 |
| | 3. Modifications of Roberts' Theory | A-7 |
| | 4. FORTRAN IV Soil Erosion Program | A-8 |
| | 5. Example FORTRAN IV Soil Erosion Calculations | A-28 |
| B | JET TURNING ANGLE | B-1 |
| C | PARTICLE TRAJECTORIES | C-1 |

ILLUSTRATIONS

| | | Page |
|-----|--|------|
| 1. | Variations of Surface Pressure With Nozzle Height (vacuum expansion) | 7 |
| 2. | Variation of Gas Radial Velocity Along the Surface Height (vacuum expansion) | 8 |
| 3. | Variation of Retro-Rocket Exhaust Gas Density Along the Surface (vacuum expansion) | 9 |
| 4. | Variation of Dynamic Pressure With Nozzle Height (vacuum expansion) | 10 |
| 5. | Variation of Surface Pressure With Nozzle Height ($n = 2.15$) | 12 |
| 6. | Variation of Gas Radial Velocity Along the Surface With Nozzle Height ($n = 2.15$) | 13 |
| 7. | Variation of Retro-Rocket Exhaust Gas Density Along the Surface ($n = 2.15$) | 14 |
| 8. | Variation of Dynamic Pressure With Nozzle Height ($n = 2.15$) | 15 |
| 9. | Variation of Maximum Soil Erosion Rate With Soil Cohesion and Particle Size (nozzle height = 5 ft, vacuum expansion) | 17 |
| 10. | Erosion Profile in a Cohesionless Soil for Various Engine Thrust Cutoff Heights (300 micron diameter soil particles, vacuum expansion) | 18 |
| 11. | Erosion Profile for Various Engine Thrust Cutoff Heights (300 micron diameter particles, 0.072 psf cohesion, vacuum expansion) | 19 |
| 12. | Erosion Profile in a Cohesionless Soil for Various Engine Thrust Cutoff Heights (50 micron diameter soil particles, vacuum expansion) | 20 |
| 13. | Erosion Profile in a Cohesionless Soil for Various Engine Thrust Cutoff Heights (10 micron diameter soil particles, vacuum expansion) | 21 |
| 14. | Erosion Profile in a Cohesionless Soil for Various Engine Thrust Cutoff Heights (300 micron diameter soil particles) ($n = 2.15$) | 23 |

ILLUSTRATIONS (continued)

| | Page |
|---|------|
| 15. Erosion Profile for Various Engine Thrust Cutoff Heights (300 micron diameter particles, 0.072 psf cohesion, $n=2.15$) | 24 |
| 16. Variation of Debris Impact Point With Particle Diameter and Engine Thrust Cutoff Height (Cohesionless Soil) | 27 |

1. SUMMARY

An analytical investigation was conducted to estimate the Martian surface loadings, soil erosion and the distances that soil debris is ejected as a result of the firing of the terminal descent rocket engine during a landing on the Martian surface. Theoretical surface loadings exhaust gas densities were computed for engine heights of 5, 10, 15, and 20 feet for the system parameters provided by Jet Propulsion Laboratories (JPL). Soil erosion rates and crater profiles were computed for Martian soils composed of 10, 50, and 300 micron diameter particles for cohesionless and cohesive soils. The erosion profile data are based on a 5 ft/sec vertical descent speed and engine thrust cutoff heights of 5, 10, 15, and 20 feet above the Martian surface. Data are also presented showing the distances along the surface that soil debris may be displaced because of soil erosion.

The computed data indicated the maximum surface excess pressure caused by gas impingement on the surface to be about 0.081 psi at the lowest nozzle height of 5 feet. This pressure is on the order of the estimated ambient pressure of 0.0726 psi provided by JPL at the Martian surface. The maximum jet gas density along the surface is about 10^{-6} slugs/ft³, which is smaller than the ambient density of about 7×10^{-5} slugs/ft³ estimated from the ambient pressure data provided by JPL. *5 in. nozzle = 0.0726 psi*

The data further indicate soil erosion will be quite small and, in general, negligible. Maximum erosion depth occurs for a soil composed of 300 micron diameter particles for the lowest thrust cutoff height of 5 feet. In a cohesionless soil, the maximum erosion depth is about 0.02 inch. Jet focusing, because of the Martian ambient pressure, may cause deeper erosions. Erosion depth data obtained for an estimate of the focusing effect indicated the maximum erosion may be increased from 0.02 to 0.05 inch. For the 10 and 50 micron diameter particles and the soil cohesion values provided by JPL, the gas viscous shear stresses were less than the soil restraint capability and therefore, no erosion takes place. If the soil is considered completely cohesionless, some erosion does occur, but the depths are smaller than in the soil composed of 300 micron diameter particles.

The surface debris displaced in a cohesive soil extends out to about 24 feet (about the radius of the erosion profile). For the cohesionless soils, the small diameter particles are accelerated to a large fraction of the gas velocity and may be displaced to about 120 feet from the stagnation point. However, if the local variations of the surface are such that soil particles depart from the surface at angles much steeper than the slope of the erosion crater, they could be displaced to much larger distances. Theoretically, at the entrained velocities of the 300 micron diameter particles and a departure angle of 15 degrees, the ballistic trajectory in a perfect vacuum would displace them about 5000 feet. Nevertheless, the Martian atmosphere would significantly reduce this range. Based on the theory developed in Appendix C and the estimated value of the drag coefficient and Martian atmospheric density, atmosphere drag would reduce the range to about 1400 feet. Most likely, such ranges are extreme upper bounds, and a more reasonable range for debris displacement may be more nearly 100 feet from the stagnation point. It should be noted that debris ejected from the lunar surface, during the translational maneuver on Surveyor VI, did not indicate any large surface erosions nor ejection of debris to large distances. During that maneuver, the predicted surface loadings were at least an order of magnitude higher than those predicted here during the descent to the Martian surface, primarily because the Surveyor vernier engine was much closer to the surface.

2. INTRODUCTION

When retro-rocket engines are used to produce the braking force required to effect a soft landing on the Martian surface, the exhaust gases produce surface loadings which may cause surface erosion, the ejection of surface debris, and also the diffusion of exhaust gases into the porous surface. The amount of erosion depends on the magnitude of the erosive forces caused by the gas, and the resistance of the surface to such erosive forces. A theoretical formulation of this phenomena was considered in References 1 and 2 for a rocket engine thrusting in the near perfect vacuum found on the moon while the jet gases impinge perpendicularly onto a surface composed of soil particles. The gas flow field created by the interaction of the impinging gases and soil surface is axisymmetric about the stagnation point, and the corresponding radial flow of the gas along the soil surface produces shear stresses on the soil. If these shear stresses exceed the shear resistance of the soil, soil particles become entrained in the flowing gas and are transported in the direction of flow, thereby forming an erosion crater in the soil. Eventually the (entrained) soil particles fall back to the surface under the influence of gravity.

Since the gravitational acceleration field is higher on Mars than on the Moon, the resistance to erosion caused by friction between soil particles is larger on Mars. On the other hand, the finite, although small, atmosphere on Mars may cause a focusing of the jet exhaust gases and thereby produce larger erosive forces on the Martian surface than would be developed by the same engine in the lunar environment. The specific dependence of surface loadings on ambient pressure is not known and is being investigated experimentally at the present time by a joint effort of JPL and Langley Research Center (LRC).

The work presented in this investigation uses the theory in References 1 and 2 to make an engineering assessment of the soil erosion during touchdown on Mars. Since it is recognized the possibility exists that the finite atmosphere existing on Mars will cause a focusing of the jet gases and influence soil erosion, a modification was made to the theory by the introduction of an additional nondimensional parameter, n (Appendix A). The validity of this procedure and the value of the nondimensional parameter can be determined when data from the current test program become available.

The next section presents data showing the surface loadings caused by the retro-rocket gases at 5, 10, 15, and 20 foot nozzle heights above the Martian surface for vacuum conditions and a case where jet focusing occurs. Data are also presented showing surface erosion produced by the gas shear stresses and data concerning the distances debris is ejected from the erosion craters.

3. RESULTS

Roberts' theory (References 1 and 2) forms the basis for the soil erosion analyses conducted in this study. The governing differential equations are presented and discussed in Appendix A along with a digital computer program listing for effecting their solution. Essentially, Roberts' theory of soil erosion is developed in two parts. The first part consists of a formulation of the forces acting on a soil surface due to the impinging retro-rocket gases. In the second part, a partial differential equation is derived which describes the rate at which soil is eroded from the surface under the action of the surface loads.

Roberts' theory was used first to determine the gas pressure loadings acting on the soil surface and then to determine the soil erosion profiles for variations in the system parameters. Finally, these results in conjunction with the particle trajectory theory presented in Appendix C were used to estimate the range the soil debris would be ejected radially. The results of these computations are presented in this section for the engine and soil parameters listed in Tables 1 and 2.

Table 1. Engine Parameters

| | | |
|--|--------------------|-------------------|
| Nozzle exit Mach number, M_e | 3.98 | |
| Nozzle exit radius, r_e (ft) | 0.389 | ≈ 4.67 in |
| Nozzle exit pressure, p_e (psia) | 0.1787 | |
| Gas constant, R (ft ² /sec ² °R) | 2310 | |
| Gas specific heat ratio, γ | 1.252 | |
| Thrust, F (lb) | 213 | |
| Expansion ratio, ϵ | 20 | |
| Conical nozzle divergence half angle, (deg) | 15 | |
| Chamber pressure, p_c (psia) | 41.7 | |
| Chamber temperature, T_c (°F) | 5670 | |
| Chamber viscosity, μ_c (lb-sec/ft ²) | 1×10^{-6} | |
| Descent rate, V_v (ft/sec) | 5 | |

$$d_c = 2.0876 \text{ in}$$

Table 2. Martian Atmospheric and Soil Parameters

| | |
|---|-------------------|
| Ambient pressure, p_o (psia) | 0.0726 |
| Acceleration of gravity, g (ft/sec ²) | 12.3 |
| Local surface slope, (deg) | 0 |
| Soil particle mass density, σ (slugs/ft ³) | 5.81 |
| Soil particle volume concentration, c (percent) | .5 (50.) |
| Soil internal friction angle, α (deg) | 34 |
| Soil particle diameter, D (microns) | 10, 50, 300 |
| Soil particle cohesion, τ_{coh} (psf) | 1950, 15.5, 0.072 |

In Table 1, the pseudo chamber pressure was computed from the exit pressure p_e , specific heat ratio γ and mach number M_e from the formula

$$p_c = p_e \left[1 + .5 (\gamma - 1) M_e^2 \right]^{\frac{\gamma}{\gamma - 1}}$$

The soil cohesion values listed in Table 2 were those prescribed by JPL for use in the study. Conservative calculations of erosion were also performed for a cohesionless soil. The values of cohesion of 1950 and 15.5 lb/ft² for the 10 and 50 micron-diameter particles were so large that, theoretically, no soil erosion should occur for soils having the particle diameters listed.

3.1 Surface Loadings

Theoretical surface loading data predicted by the theory in Appendix A (vacuum expansion) are shown in Figures 1 through 4 for nozzle heights of 20, 15, 10 and 5 feet. Figure 1 shows the increment in surface pressure caused by the impinging gases. The figure indicates that the maximum excess surface pressure is .081 psi for a nozzle height of 5 feet. If this pressure is added to the existing ambient pressure of .0726 psi, the pressure would be about .154 psia. The figure indicates that the impinging gas differential pressures are generally less than the ambient pressure; and for all nozzle heights, are less than 10 percent of the ambient pressure at radial distances larger than about 5.5 feet from the stagnation point.

Figure 2 shows the theoretical radial velocity of the gas, u , along the surface for the four nozzle heights. The figure indicates that at the 5 foot

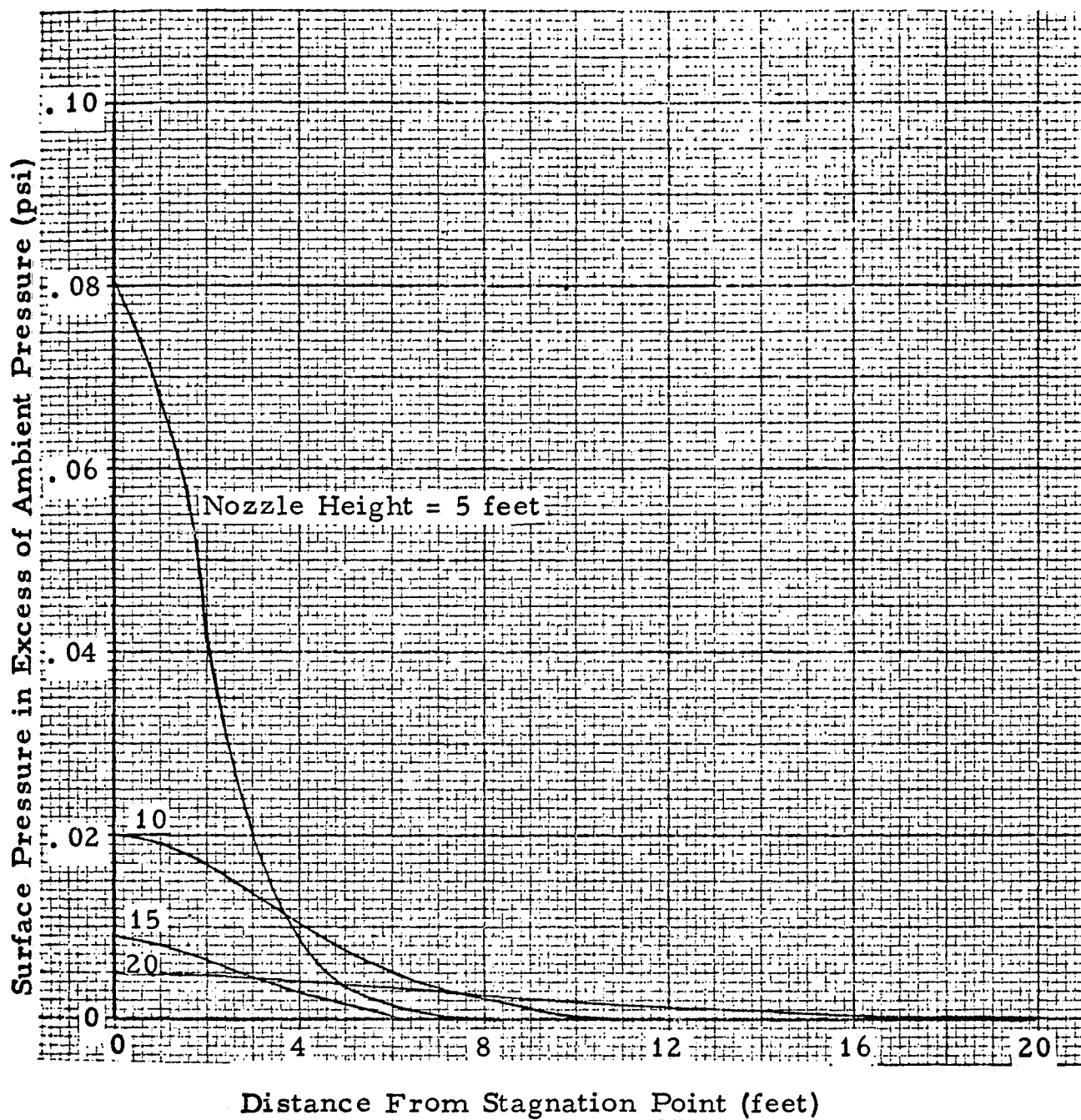


Figure 1. Variations of Surface Pressure With Nozzle Height (Vacuum Expansion)

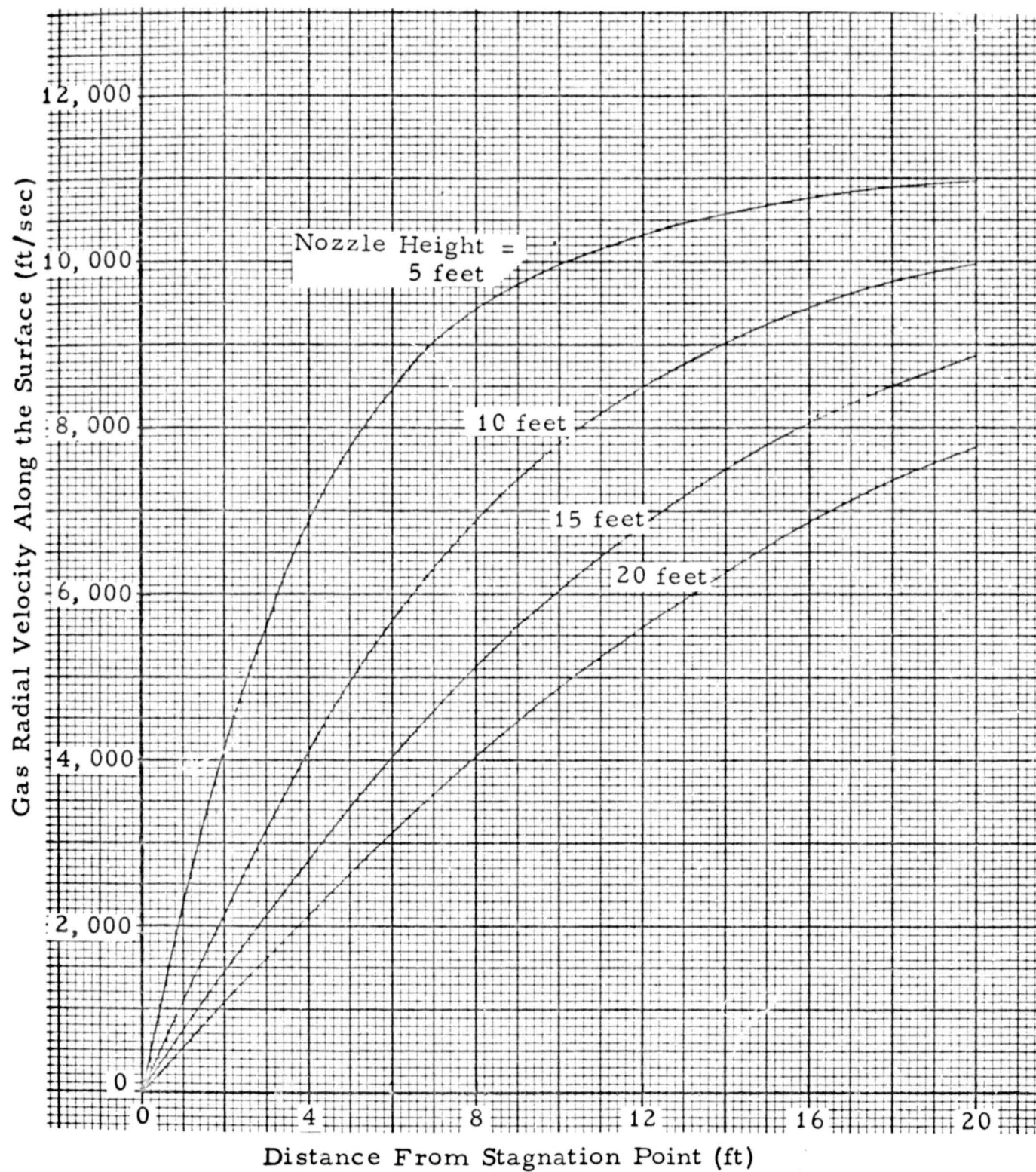


Figure 2. Variation of Gas Radial Velocity Along the Surface With Nozzle Height (Vacuum Expansion)

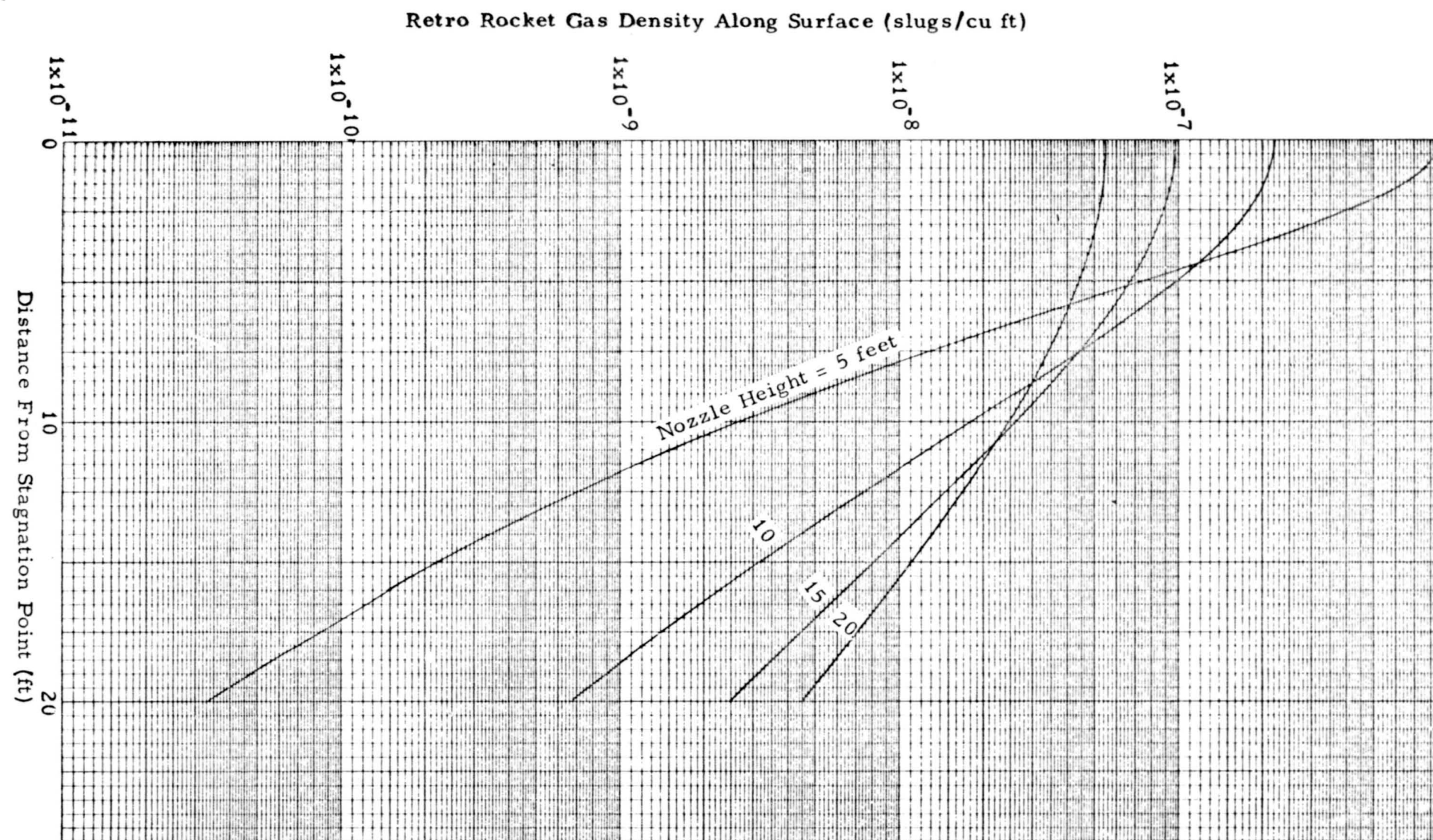


Figure 3. Variation of Retro-Rocket Exhaust Gas Density Along the Surface (Vacuum Expansion)

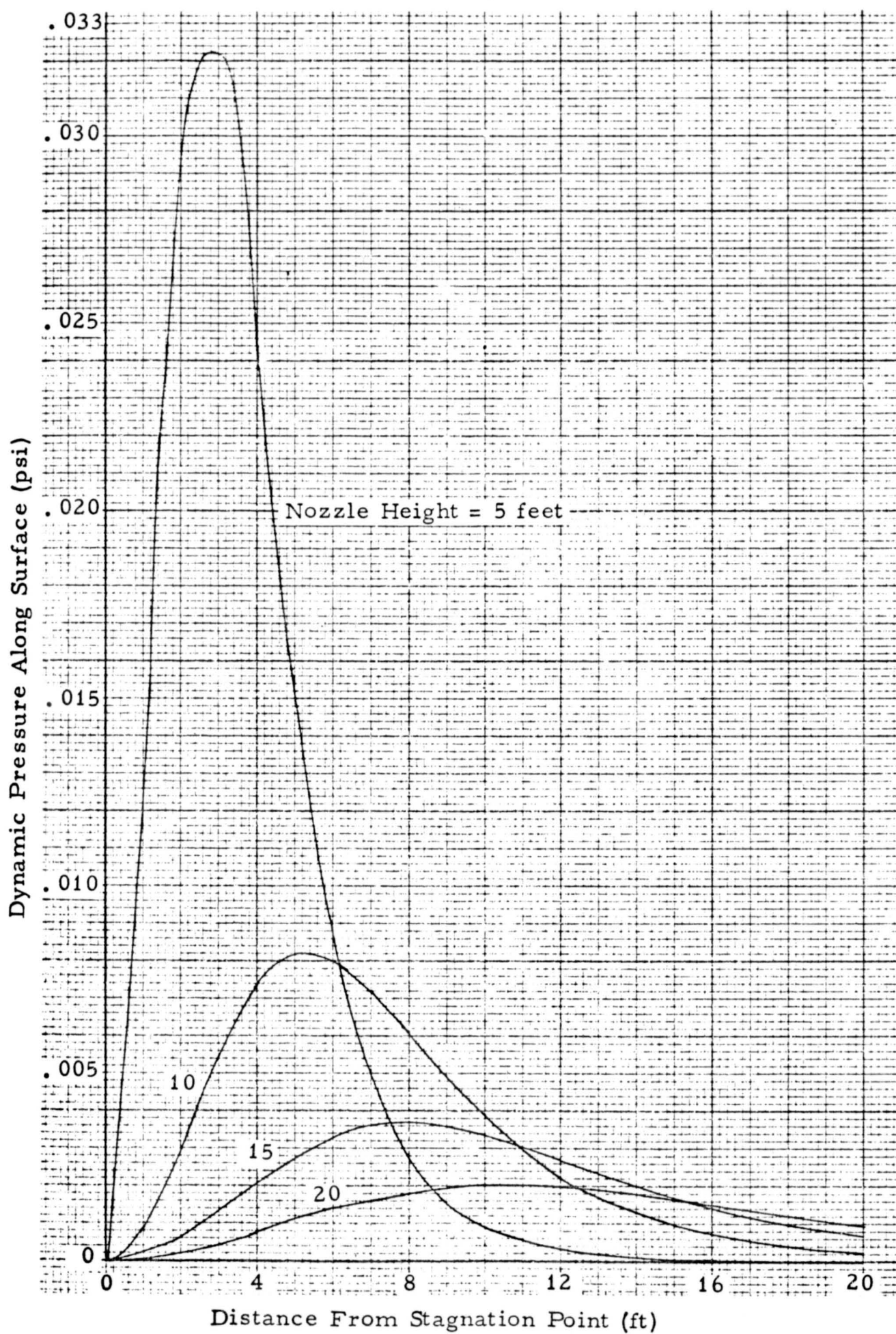


Figure 4. Variation of Dynamic Pressure With Nozzle Height (Vacuum Expansion)

nozzle height the radial velocity is about 11,000 ft/sec at a distance of 20 feet from the stagnation point. Hence, at this point the gas has almost attained the theoretical velocity of about 11,400 ft/sec to be reached at infinite distances ($p_{\infty} \rightarrow 0$).

Figure 3 shows the exhaust gas mass density ρ along the surface for the four nozzle heights. The figure indicates that the gas density decreases rapidly for increasing distances from the stagnation point.

Figure 4 shows the gas dynamic pressure q (equal to $\rho u^2/2$) along the surface for the four nozzle heights. The viscous shear stress transmitted to the soil is proportional to the dynamic pressure. The figure indicates the maximum dynamic pressure is about .0322 psi (4.64 psf). Thus, for a viscous friction coefficient $C_f = .2$ the maximum shear stress acting on the soil would be about .93 psf. Hence, if the soil restraining stress is greater than .93 psf, theoretically, no soil erosion will occur.

To provide some indication of how the Martian atmosphere may affect surface loadings, calculations were performed for a value of the focusing parameter different from $n = 1$ ($n = 1$ corresponds to expansion into a perfect vacuum). In Appendix B it was found that the jet turning angle was about 114 degrees in a vacuum and 24.6 degrees in a Martian type atmosphere. If one assumes the effective value of the jet focusing parameter n is the square root of the jet turning angles, then $n = 2.15$ and the corresponding surface loadings are as shown in Figures 5 through 8. (The assumption that the jet focusing effect can be accounted for through the single parameter n and its functional dependence on the jet turning angles must, of course, be verified when the necessary test data becomes available.)

A comparison of Figure 1 through 4 with Figures 5 through 8 indicates a value of $n = 2.15$ produces static and dynamic surface pressures about 2.5 times as large as in a perfect vacuum, and the loadings are more concentrated around the stagnation point.

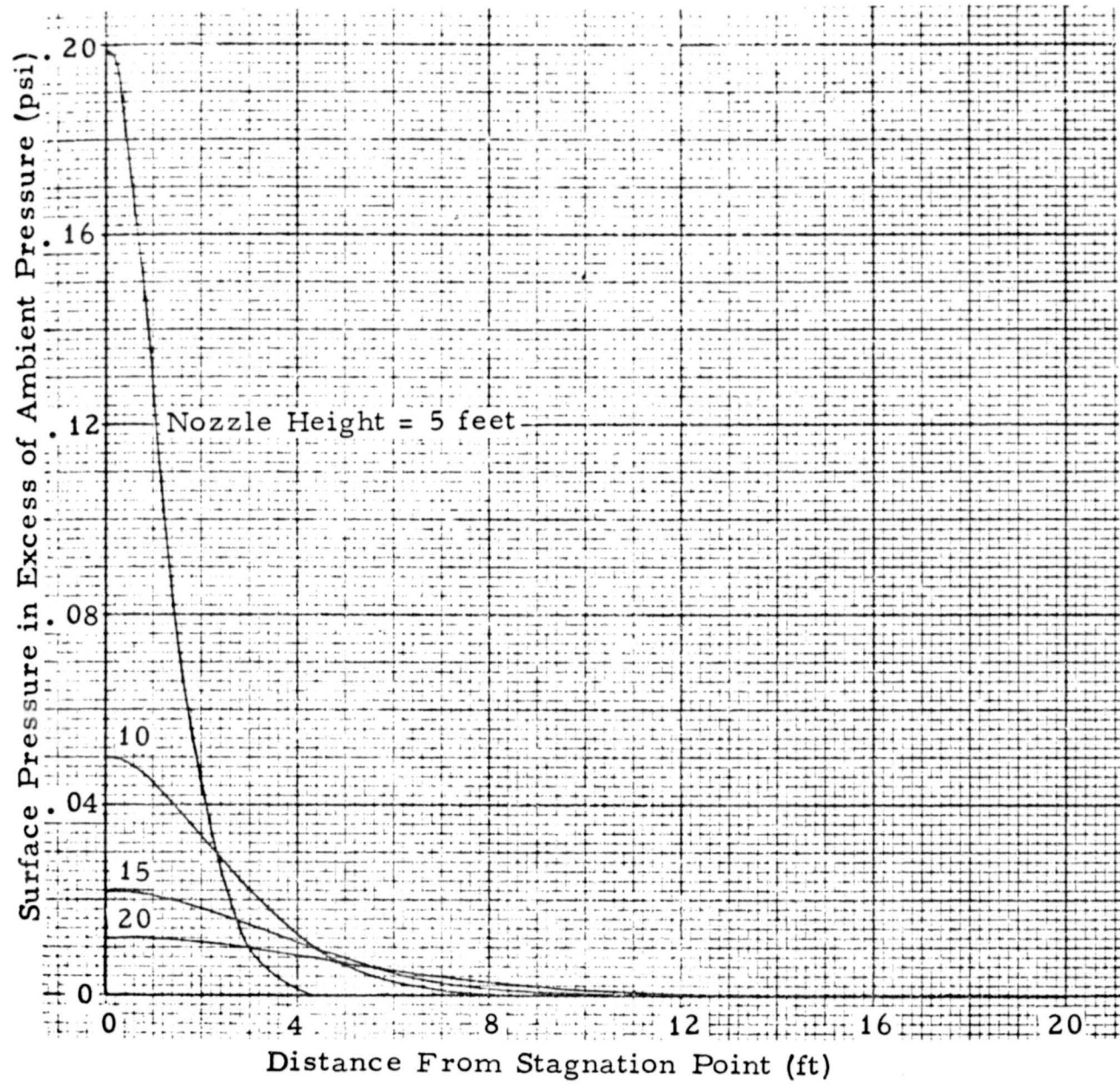


Figure 5. Variation of Surface Pressure
With Nozzle Height
($n = 2.15$)

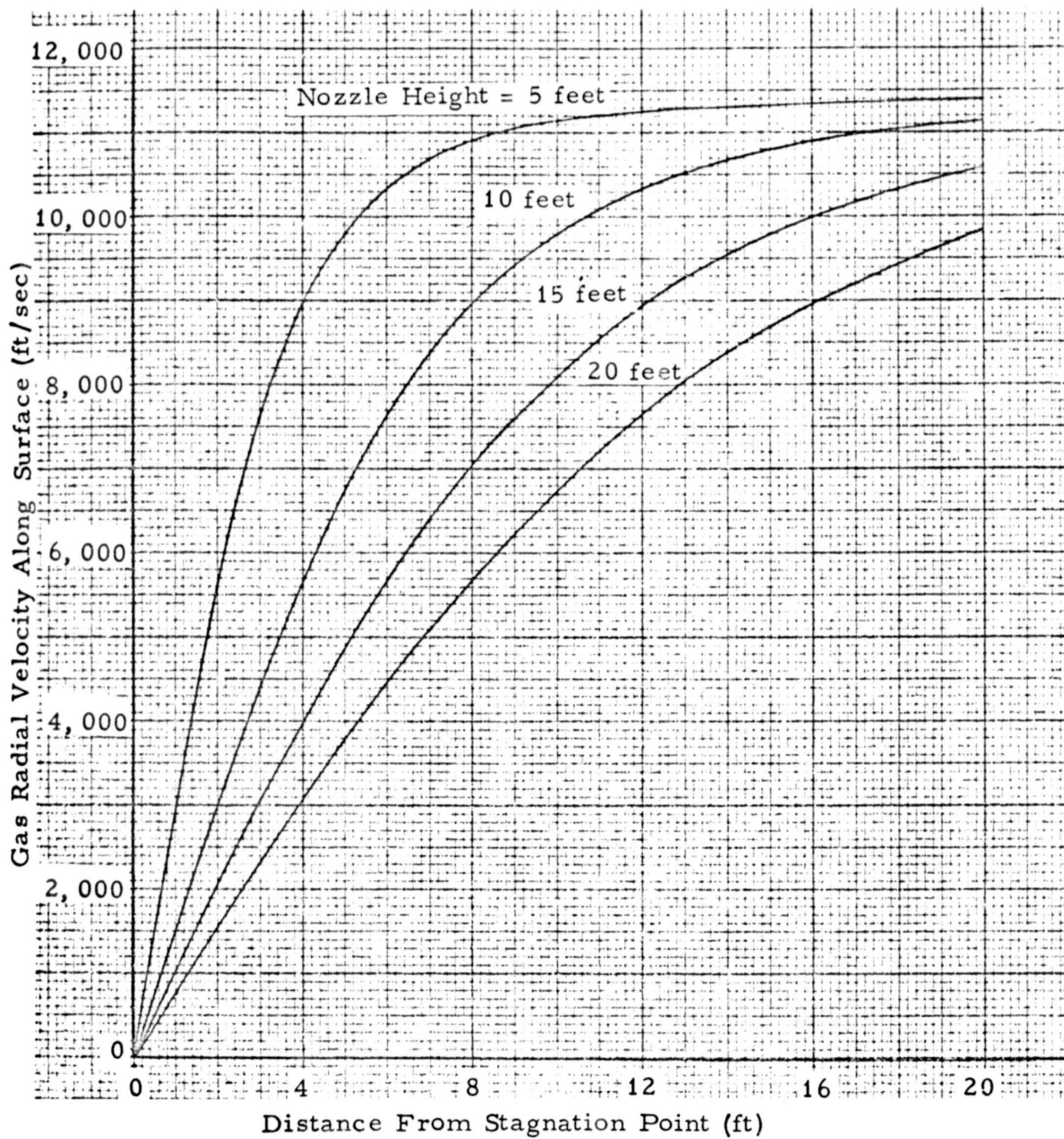


Figure 6. Variation of Gas Radial Velocity Along the Surface With Nozzle Height
($n = 2.15$)

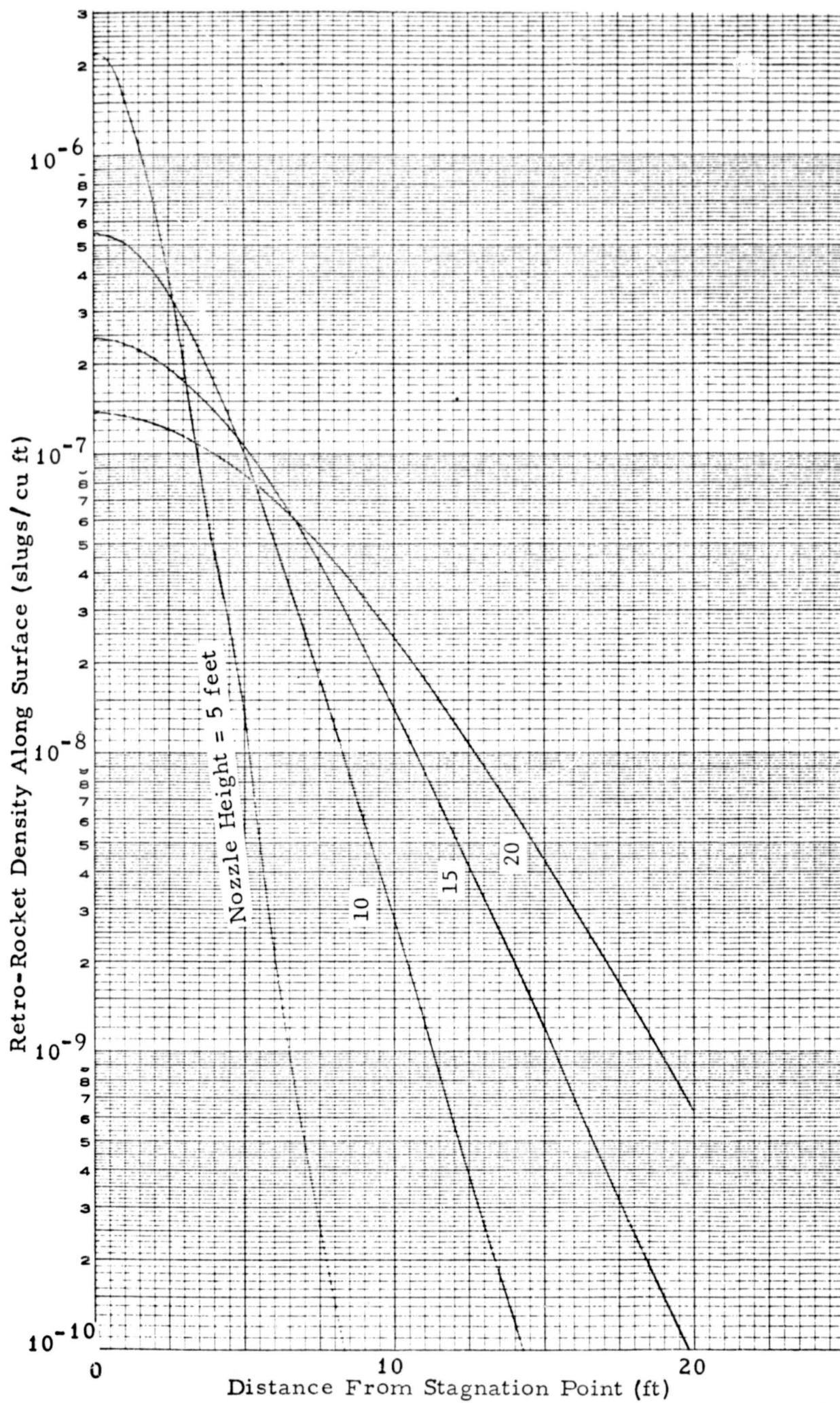


Figure 7. Variation of Retro-Rocket Exhaust Gas Density Along the Surface
($n = 2, 15$)

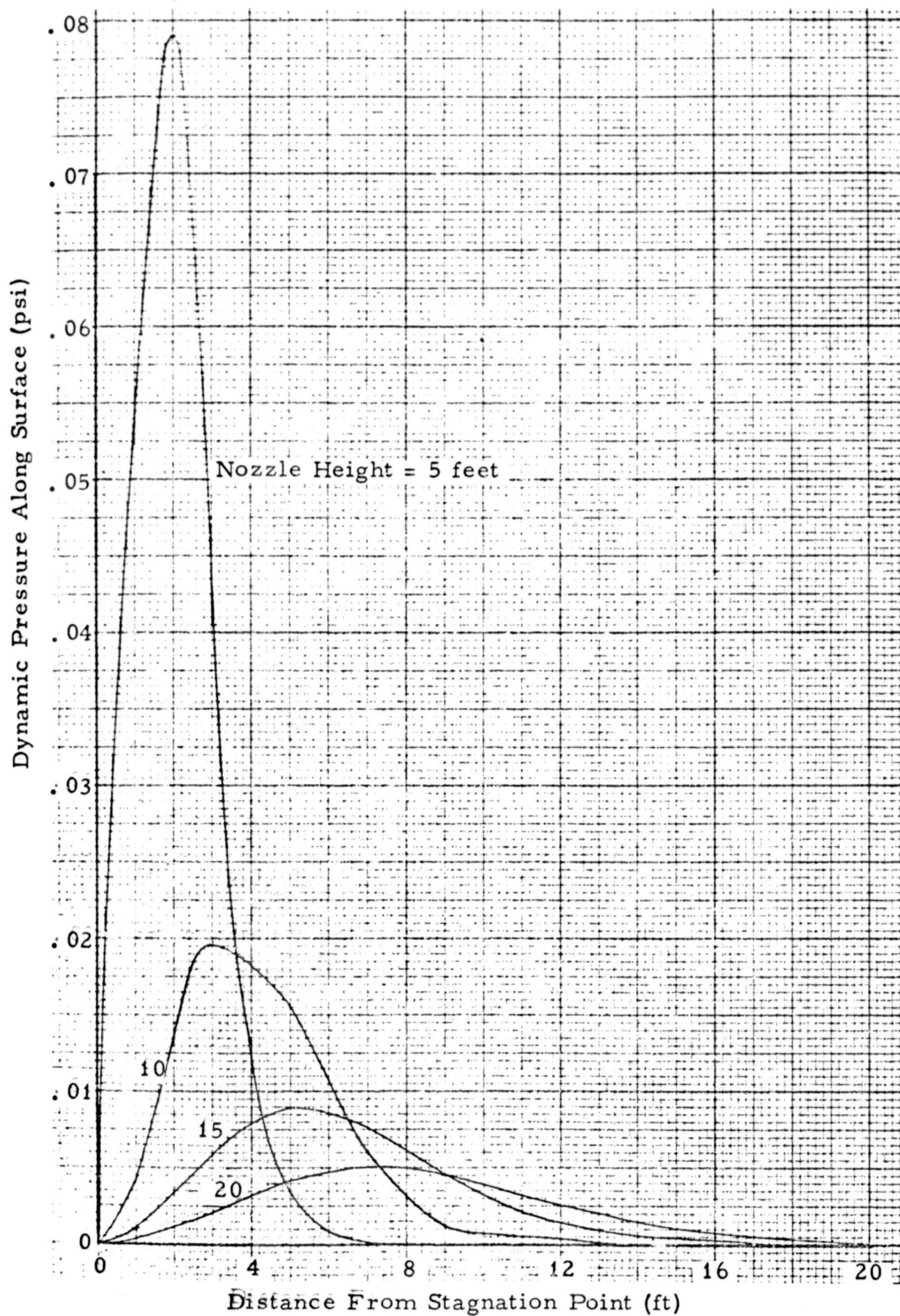


Figure 8. Variation of Dynamic Pressure
With Nozzle Height
($n = 2.15$)

3.2 Soil Erosion

Theoretical soil erosion data were computed according to the procedure in Appendix A and are presented in this section. Figure 9 shows the soil erosion rate for a range of soil cohesion for three particle diameters when the nozzle is 5 feet above the surface and expanding into a perfect vacuum. The figure indicates that no erosion should occur for any of these particle diameters for a soil cohesion larger than about .93 psf. The shear stress to be exceeded by the gas viscous forces is composed of two parts; soil cohesion and restraint offered by the internal friction. The internal friction restraint on a flat surface is $\sigma CDg \tan \alpha$, which for the 300 micron particles is about 0.021 psf. Thus, in general, this restraint is negligible compared to that offered by the soil cohesion, except in a cohesionless soil. Referring to the soil cohesion values listed in Table 2, one concludes from Figure 9 that soil erosion will not occur for the 10 and 50 micron-diameter particles for the 5 foot engine thrust cutoff height, or any higher cutoff height. However, since the listed cohesion values (based upon 0.5 psi for 30 μ) may be optimistic, conservative calculations were performed for a cohesionless soil. (For example, lunar soil cohesion estimated from Surveyor data is .02 to .05 psi, or 2.9 to 7.2 psf, for particle diameters less than the resolution of the TV camera of about .01 inch or 25 microns.) The results of these calculations are shown in Figures 10, 11 and 12.

Figure 10 shows the vacuum expansion erosion profiles for 300 micron diameter particles for engine thrust cutoff heights of 20, 15, 10 and 5 feet for a cohesionless soil.

Figure 11 shows the same data for a soil having the cohesion listed in Table 2. Observe that, even for a cohesionless soil, the maximum erosion depth is quite small and is about 0.0017 foot (0.02 inch).

Figures 12 and 13 show the vacuum expansion erosion profiles for 50 and 10 micron diameter particles for a cohesionless soil. Although no erosion should occur for the cohesion values listed in Table 2, even in a cohesionless soil, the erosion is still quite small.

A comment might be made at this point concerning the effect of particle diameter on the shear stress required to produce an erosion and the subsequent rate of erosion. An examination of the theory indicates

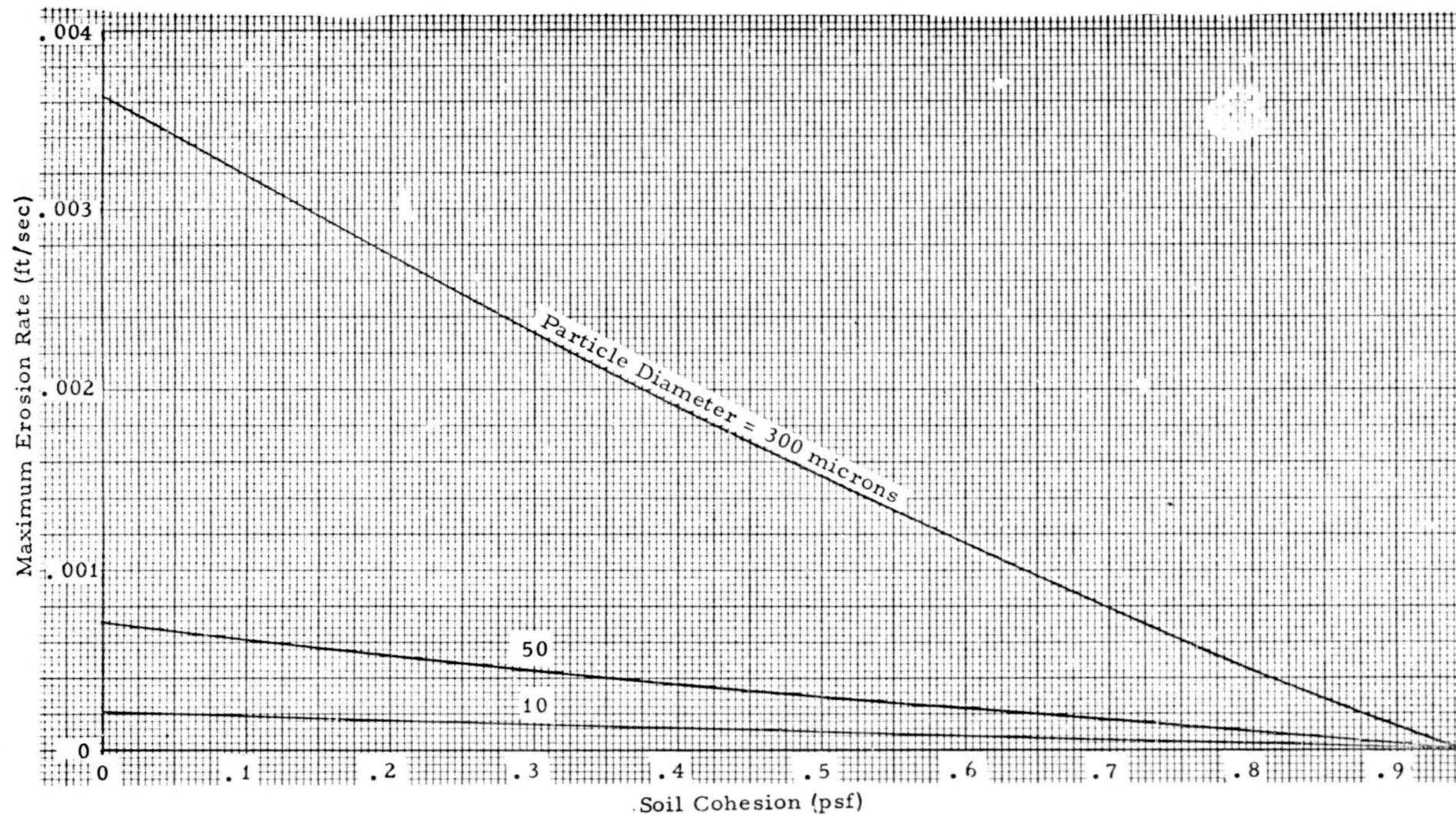


Figure 9. Variation of Maximum Soil Erosion Rate With Soil Cohesion and Particle Size (Nozzle Height = 5 ft, Vacuum Expansion)

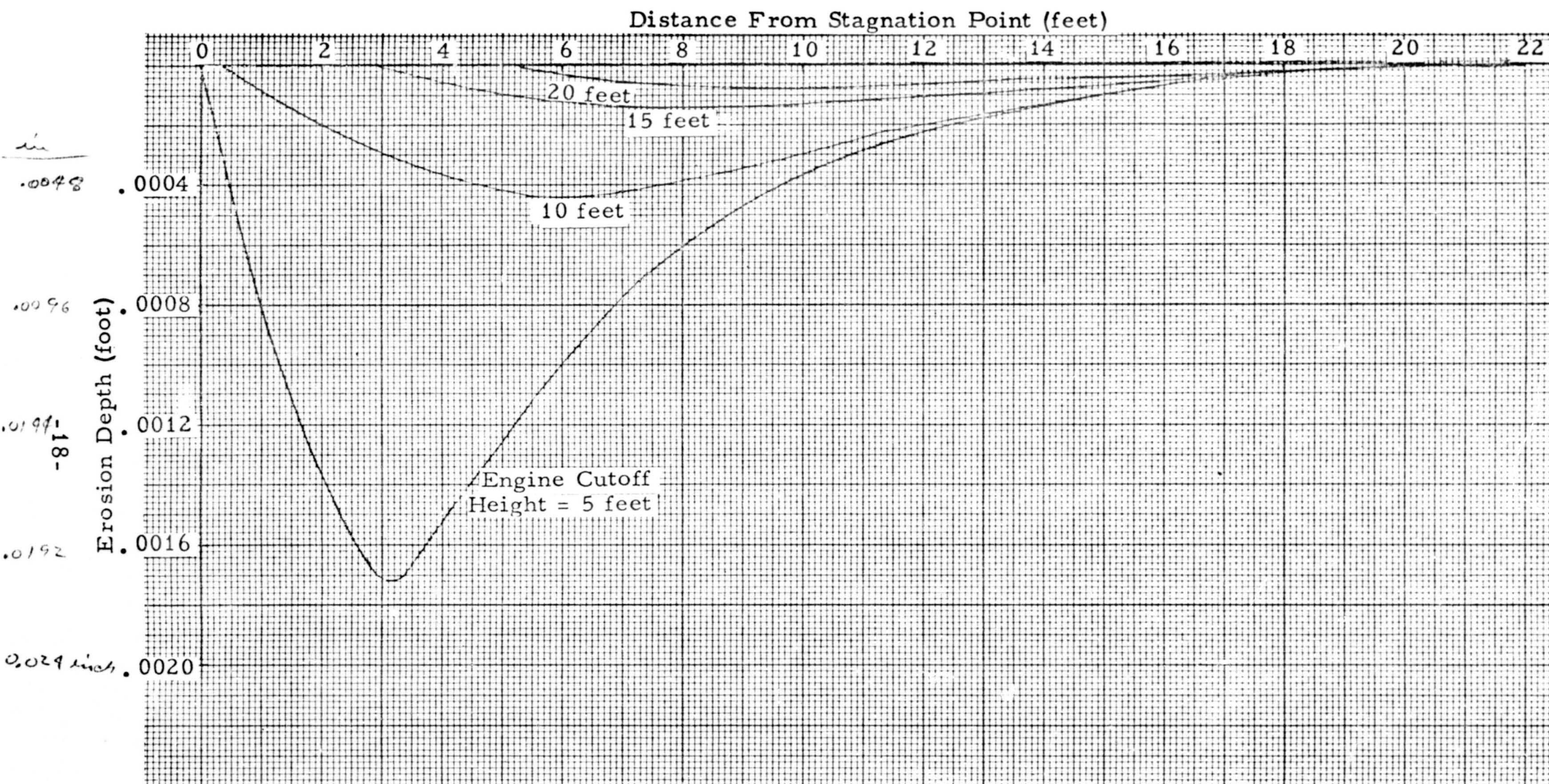


Figure 10. Erosion Profile in a Cohesionless Soil for Various Engine Thrust Cutoff Heights (300 micron diameter soil particles, vacuum expansion)

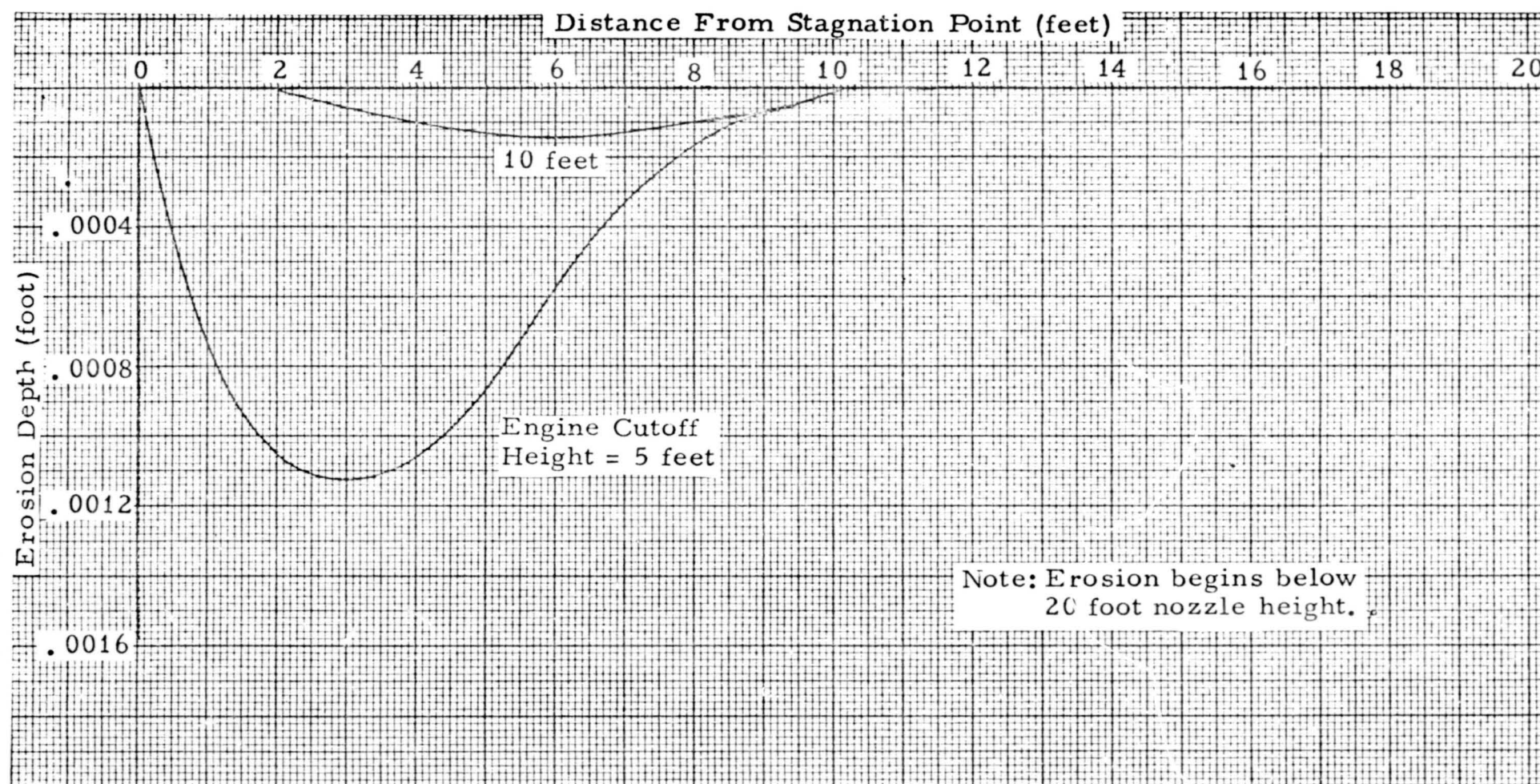


Figure 11. Erosion Profile for Various Engine Thrust Cutoff Heights
(300 micron diameter particles, 0.072 psf cohesion,
vacuum expansion)

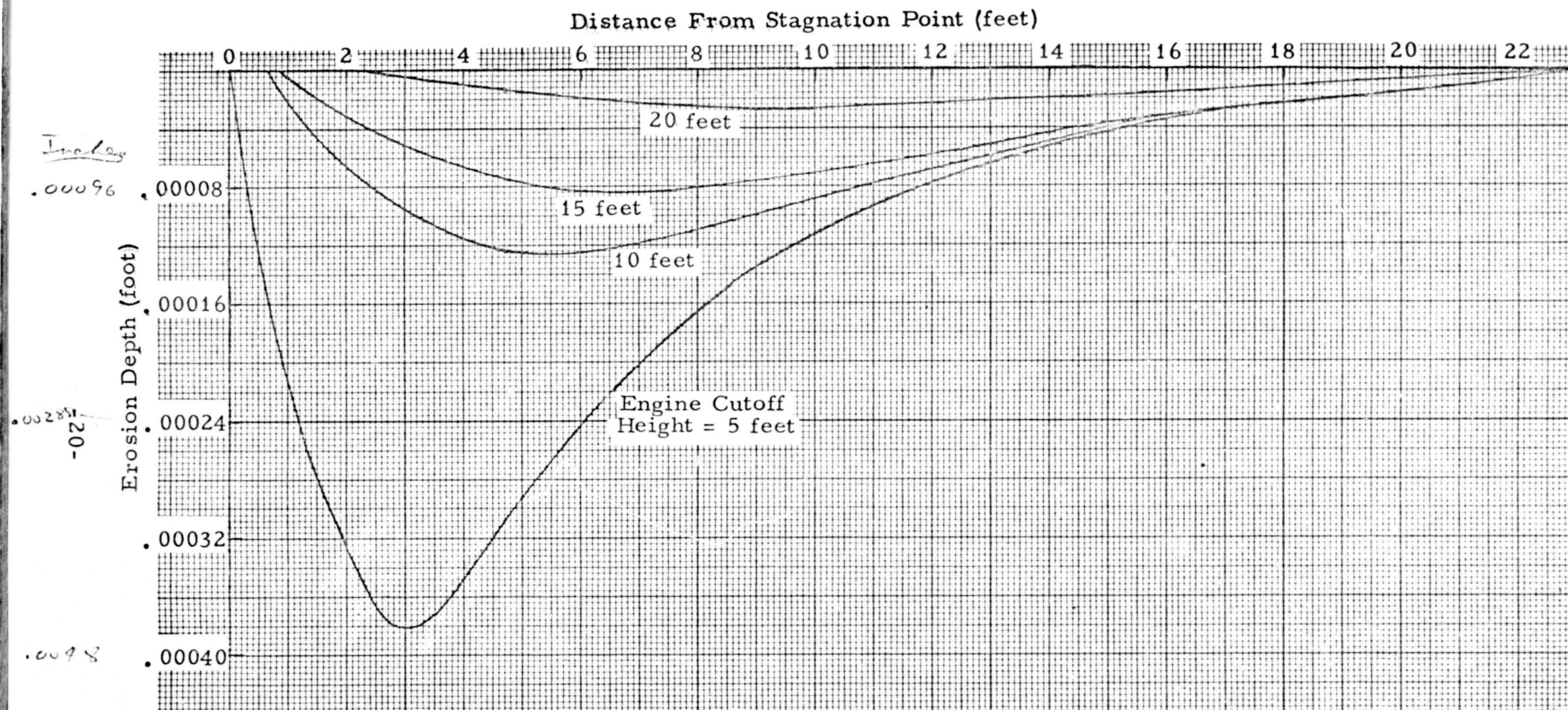


Figure 12. Erosion Profile in a Cohesionless Soil for Various Engine Thrust Cutoff Heights (50 micron diameter soil particles, vacuum expansion)

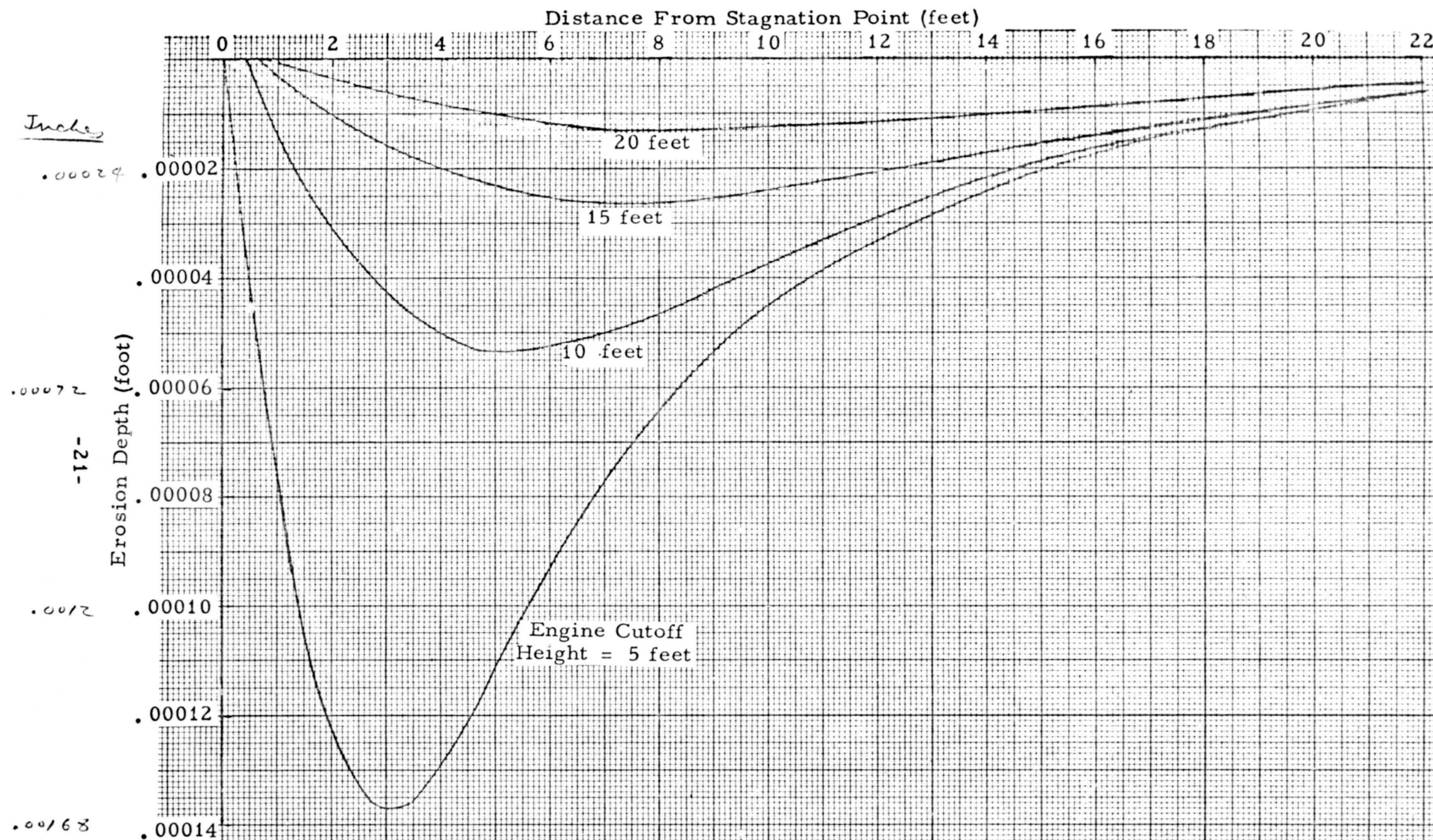


Figure 13. Erosion Profile in a Cohesionless Soil for Various Engine Thrust Cutoff Heights (10 micron diameter soil particles, vacuum expansion)

that for a fixed value of cohesion the shear stress required to produce an erosion is larger for larger diameter particles. This is because the larger the particle, the larger the soil weight; and hence, the larger the restraint offered by the soil as a result of internal friction. However, the differences in restraint are generally negligible compared to any reasonable value of soil cohesion. On the other hand, if the erosive shear stresses are in excess of the restraint offered by the soil, the larger the particle diameter, the larger the rate of erosion. This follows from the fact that the theory is based on a momentum balance between the gas particles and soil particles. Small soil particles are rapidly accelerated and provide an efficient transfer of momentum to the soil, while large soil particles attain only a small fraction of the gas velocity. Soil erosion experiments bear out this behavior and demonstrate that the erosion rate increases with increasing particle diameter until the particles become so large that the frictional restraint exceeds the viscous erosive stresses. To provide some indication of the effect of jet focusing on surface erosion, computations were also performed for the focusing parameter $n = 2.15$. The results are shown in Figures 14 and 15 for a 300 micron-diameter particle soil. The figures show the profiles for a cohesionless soil and a soil having the cohesion listed in Table 2. A comparison of Figure 14 with Figure 10 indicates the maximum erosion depth is about twice that in a perfect vacuum. But even so, it is still quite small.

3.3 Soil Particle Displacements

Because of the very small erosion for the prescribed descent to the Mars surface (even for a cohesionless soil), particles should depart from the surface at very low angles and therefore, have small lateral displacements. The low departure angles are a consequence that, theoretically, the particles leave the surface tangent to the erosion crater. Theory indicates the maximum range is traversed by particles lying between the point of maximum depth and the outer crater lip because the crater slopes are larger in this region. The distance a particle travels from the point it enters the stream depends on the local erosion crater slope and the velocity of the particle. Since a soil composed of a given particle size erodes faster than a surface having smaller particles, the local slope is greater for the larger particles, for the same exposure time to the erosive gas forces. However, the larger particles attain a much smaller

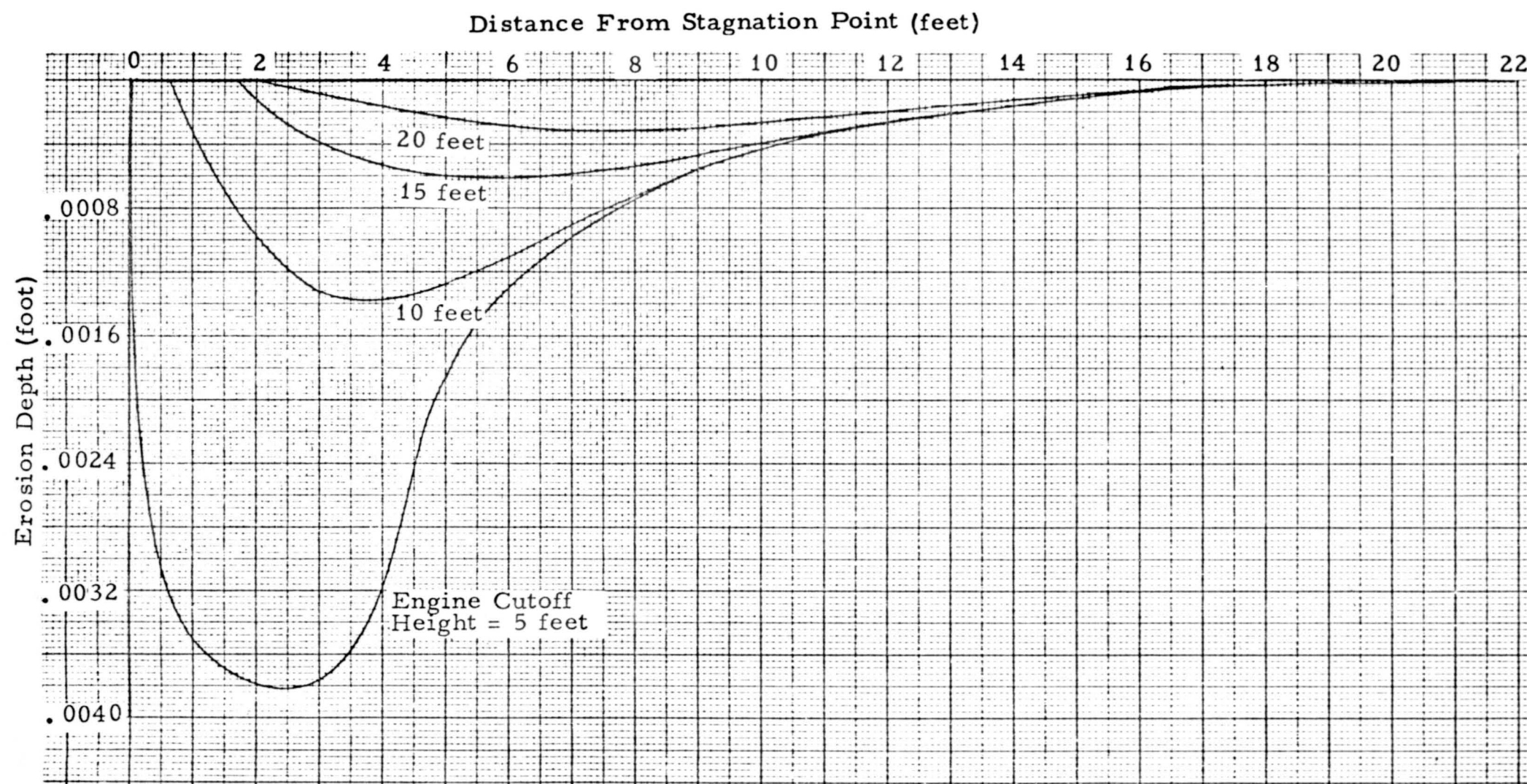


Figure 14. Erosion Profile in a Cohesionless Soil for Various Engine Thrust Cutoff Heights
(300 micron diameter soil particles)
($n = 2.15$)

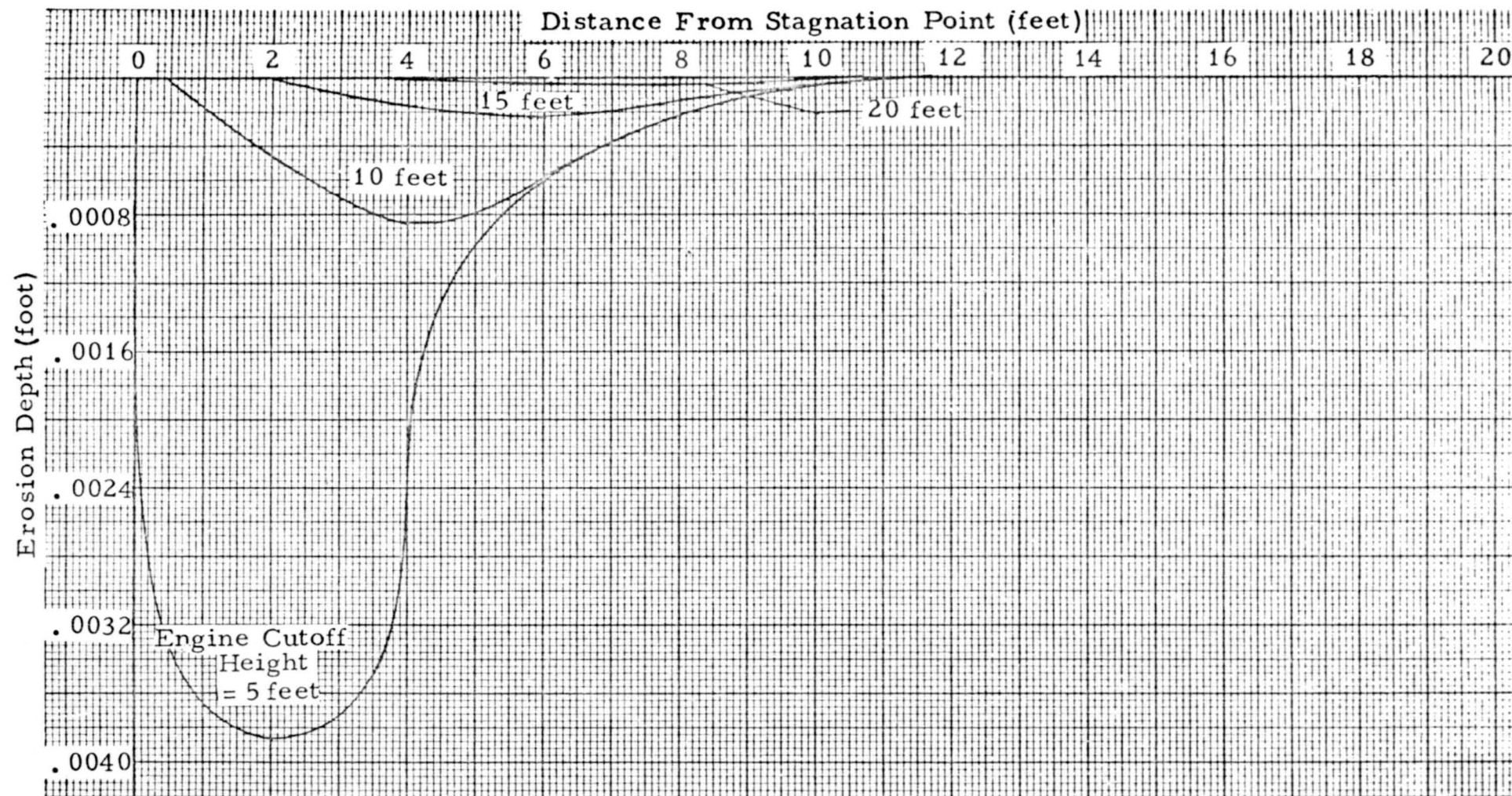


Figure 15. Erosion Profile for Various Engine Thrust Cutoff Heights
(300 micron diameter particles, 0.072 psf cohesion, $n = 2.15$)

fraction of the gas velocity than the smaller particles. Thus, the ballistic trajectory of larger particles may or may not have a longer range than the range of smaller particles. For the system parameters considered here, along with the 5 foot ^{per second} descent rate, the surface erosion and erosion crater slope are quite small. This results in a relatively small trajectory range for all soil particle diameters considered. Consequently, the surface debris is largely confined to the region in which erosion takes place. As the spacecraft descends toward the surface, the erosion region decreases in size, although erosion rate increases.

In a cohesionless soil, incipient erosion begins around nozzle heights of 170, 80 and 30 feet for the 10, 50 and 300 micron diameter particles, respectively. At these heights, the maximum viscous shearing stresses along the surface are just equal to the restraint offered by the friction between soil grains. At these incipient erosion heights, the points of maximum shear stress are at radial stations located about 93, 42 and 17 feet from the stagnation point for the 10, 50 and 300 micron diameter particles, respectively. Consider, for example, the formation of the erosion crater in a 10 micron diameter cohesionless soil. At the 170 foot nozzle height, a surface erosion begins about 93 feet from the stagnation point. As the spacecraft descends, the region in which erosion takes place moves toward the stagnation point. At engine cutoff, say at a 5 foot nozzle height, the maximum rate of erosion has moved to about 2 feet from the stagnation point. A particle that enters the gas stream just prior to engine cutoff about 7 feet from the stagnation point, where the erosion crater has an upward slope, has a ballistic range in a vacuum of about 90 feet. This range transports the particle approximately to the region where erosion first occurred during descent. Consequently, the distance debris is transported along the surface is essentially confined to the entire region in which erosion takes place during the descent period. As a result, the distance debris is deposited along the surface is essentially the same for 20, 10 or 5 foot engine thrust cutoff heights. An exception is provided by 100 micron particles for a 5 foot nozzle cutoff height. In this case, the erosion is fast enough to produce a local slope such that the ballistic trajectory of a particle located about 8 feet from the stagnation point travels about 10 feet beyond the incipient erosion point.

Results of soil particle displacements computations are summarized in Figure 16. The particle velocities and departure angles used in the calculations were those obtained from the erosion calculations. These were compared with the limiting erosion profile also obtained from the same calculations. The range plotted is the larger of these two results, which, as indicated earlier, generally was the limit of the erosion crater. It should be recalled that, if the soil cohesion is as large as listed in Table 2, no erosion of particles smaller than 50 microns in diameter should occur. Therefore, the particle displacement ranges shown for particle diameters up to 50 microns should be an extreme upper bound estimate.

Even though this theory indicates the erosion should be small and the particles displaced only small distances, one should not overlook the idealization of the theory. For example, an actual soil surface is most likely undulating, nonhomogeneous and composed of a distribution of particle sizes. The variations in local slope of the virgin surface most likely exceeds the maximum slope predicted here for the erosion crater. Hence, soil particles may depart from the surface with velocities comparable to those predicted here, but at angles larger than the crater profile makes with the horizontal. It seems quite likely they could depart from the surface at angles as large as 15 degrees. In such an event, the theory in Appendix C would predict the ranges tabulated in Table 3.

Table 3. Theoretical Range for 5 Foot Engine Cutoff Height and 15 Degree Departure Angle

| Soil Particle Diameter (microns) | Soil Particle Velocity (ft/sec) | Range (ft) | |
|----------------------------------|---------------------------------|------------|-----------------------------|
| | | Vacuum | Atmosphere ($C_D = 0.14$) |
| 10 | 6011 | 1,470,000 | 194 |
| 50 | 1861 | 141,000 | 675 |
| 300 | 350 | 4,964 | 1420 |

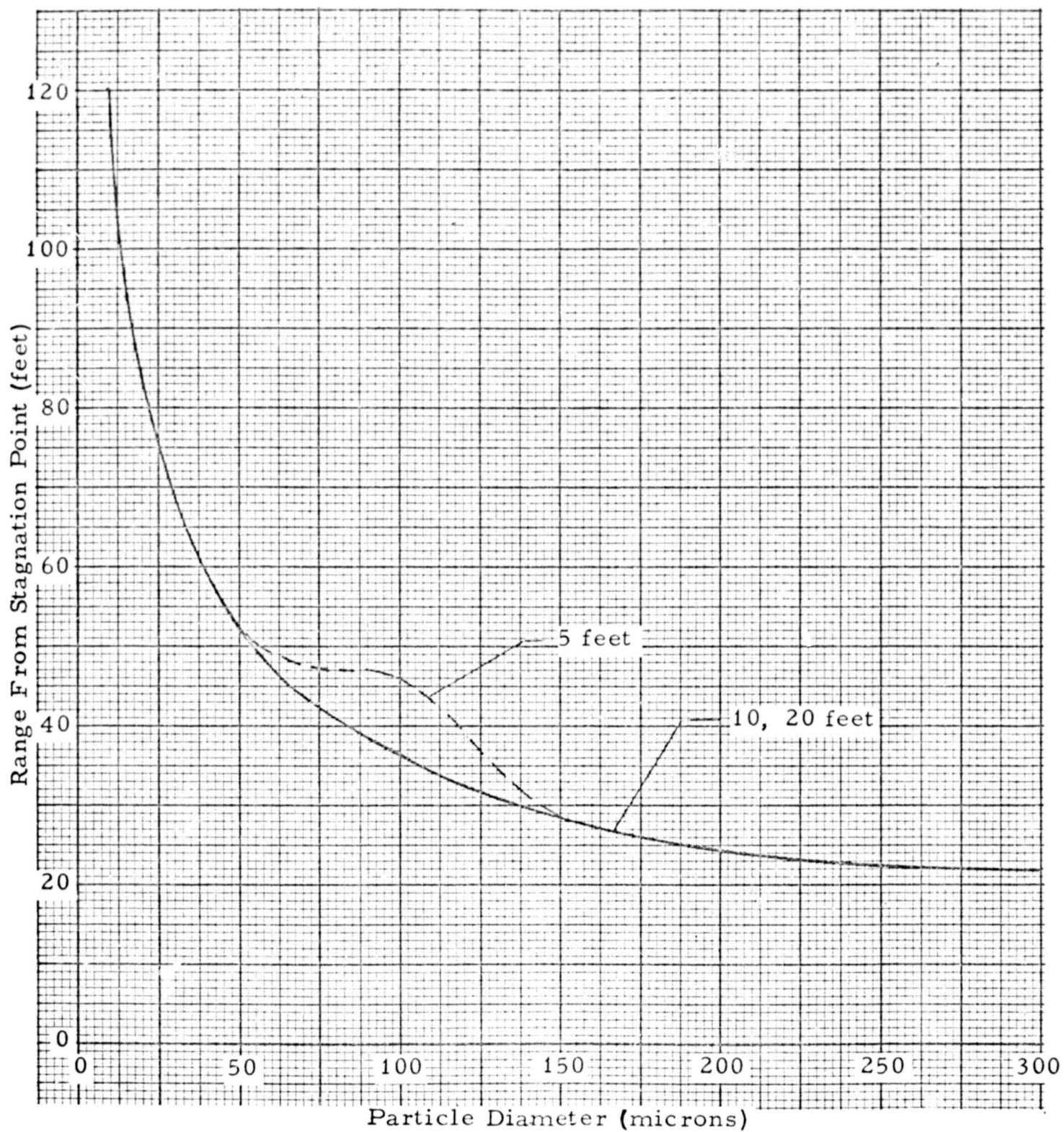


Figure 16. Variation of Debris Impact Point With Particle Diameter and Engine Thrust Cutoff Height (cohesionless soil)

These data were based on drag coefficients of 0 and 0.14 corresponding to vacuum and atmospheric conditions. The density of the Martian atmosphere used in these calculations was estimated from the ambient pressure of 0.0726 psi (10.45 psf). The estimate was made based on CO₂ whose molecular weight is 44 and at a temperature of 128°R. The gas constant and density were then computed to be

$$R = \frac{49686}{44} = 1130 \text{ ft}^2/\text{sec}^2 \text{ } ^\circ\text{R}$$

$$\rho = \frac{P}{RT} = \frac{10.45}{(1130)(128)} = 7.22 \times 10^{-5} \text{ slugs/ft}^3$$

These values indicate the range could far exceed those shown in Figure 16. The tabulated results in Table 3 reflect the fact that small-diameter particles are readily accelerated by the gas stream, and the subsequent ballistic trajectory in a vacuum would have an extremely large range. However, these same small particles would be readily decelerated by the drag forces produced by the Martian atmosphere. It should be emphasized that the ranges computed for atmospheric conditions are the result of certain basic assumptions. First, it assumes the retarding aerodynamic force is proportional to the square of the particle velocity. This seems reasonable, but may only be valid over a limited portion of the entire velocity range. Second, even if the velocity square drag law is valid, the corresponding drag coefficient may vary with particle diameter and velocity (or Reynolds number). If this is the case, the estimated value of $C_D = 0.14$ from bullet range data, which have diameters much larger than the soil particles, may be in error. If the drag coefficient was significantly smaller than the value used here, the ranges in the presence of an atmosphere would approach that in a vacuum condition.

In summary, erosion calculations indicate surface erosion to be negligible for the range of parameters considered in this study, even for a cohesionless Martian soil. The corresponding range debris is displaced laterally along the surface should be less than 30 feet from the stagnation point, but may be as large as 120 feet if the soil is cohesionless. On the other hand, one cannot rule out the possibility that the local surface roughness may cause some particles to be displaced to larger distances. The

These data were based on drag coefficients of 0 and 0.14 corresponding to vacuum and atmospheric conditions. The density of the Martian atmosphere used in these calculations was estimated from the ambient pressure of 0.0726 psi (10.45 psf). The estimate was made based on CO₂ whose molecular weight is 44 and at a temperature of 128°R. The gas constant and density were then computed to be

$$R = \frac{49686}{44} = 1130 \text{ ft}^2/\text{sec}^2 \text{ } ^\circ\text{R}$$

$$\rho = \frac{P}{RT} = \frac{10.45}{(1130)(128)} = 7.22 \times 10^{-5} \text{ slugs/ft}^3$$

These values indicate the range could far exceed those shown in Figure 16. The tabulated results in Table 3 reflect the fact that small-diameter particles are readily accelerated by the gas stream, and the subsequent ballistic trajectory in a vacuum would have an extremely large range. However, these same small particles would be readily decelerated by the drag forces produced by the Martian atmosphere. It should be emphasized that the ranges computed for atmospheric conditions are the result of certain basic assumptions. First, it assumes the retarding aerodynamic force is proportional to the square of the particle velocity. This seems reasonable, but may only be valid over a limited portion of the entire velocity range. Second, even if the velocity square drag law is valid, the corresponding drag coefficient may vary with particle diameter and velocity (or Reynolds number). If this is the case, the estimated value of $C_D = 0.14$ from bullet range data, which have diameters much larger than the soil particles, may be in error. If the drag coefficient was significantly smaller than the value used here, the ranges in the presence of an atmosphere would approach that in a vacuum condition.

In summary, erosion calculations indicate surface erosion to be negligible for the range of parameters considered in this study, even for a cohesionless Martian soil. The corresponding range debris is displaced laterally along the surface should be less than 30 feet from the stagnation point, but may be as large as 120 feet if the soil is cohesionless. On the other hand, one cannot rule out the possibility that the local surface roughness may cause some particles to be displaced to larger distances. The

possibility exists, although most likely quite remote, that some particles could have ranges as large as, or larger than, 1400 feet from the stagnation point.

REFERENCES

1. Leonard Roberts, "The Action of a Hypersonic Jet on a Dust Layer, " Presented at the Thirty-First Annual Meeting of the Institute of the Aerospace Sciences, January 1963.
2. Leonard Roberts, "The Interaction of a Rocket Exhaust with the Lunar Surface, " Presented at a Specialists' Meeting on Fluid Dynamic Aspects of Space Flight, under the Sponsorship of the Fluid Dynamics Panel of the Advisory Group for Aeronautical Research and Development, Marseilles, France, April 20-24, 1964.
3. R. E. Hutton, "An Investigation of Soil Erosion and Its Potential Hazard to LM Lunar Landing, " Prepared for the National Aeronautics and Space Administration, Manned Spacecraft Center, Houston, Texas, TRW Systems Engineering Mechanics Report EM 16-11, October 1966.
4. E. K. Latvala, "Spreading of Rocket Exhaust Jets at High Altitudes, " AEDC-TR-59-11, June 1959.
5. H. W. Liepman, A. Roshko, Elements of Gasdynamics, John Wiley & Sons, New York, 1960.
6. J. S. Hatcher, Hatcher's Notebook, Stackpole Company, Harrisburg, Pennsylvania, 1947.

APPENDIX A. ROBERTS' THEORY

In References 1 and 2 Roberts first develops a description of the gas flow field caused by the gases emanating from a nozzle located a distance h above a flat soil surface. He then develops a theory describing the rate the soil surface erodes under the action of the gas viscous forces generated while the gas flows from the stagnation point radially outward along the soil surface.

Initially, Roberts make an assumption regarding the spatial variation in gas density as it emanates from the nozzle. Then, by applying perfect gas theory and boundary layer theory, analytical expressions are developed to describe the gas radial velocity, static and dynamic pressures along the soil surface, and viscous shear forces acting on the soil. An impulse-momentum relation is then postulated to exist in the form

$$(\Delta m) v = A (\tau - \tau^*) \Delta t \quad (A1)$$

which relates the momentum change of soil mass Δm to the impulse caused by the gas viscous shear forces. In Equation (A1), v is the velocity imparted to the element of soil mass, A is the cross-sectional area of the element of mass, τ is the viscous shear stress acting on the soil mass, and τ^* is the soil restraining shear force due to friction and cohesion between the soil grains that must be exceeded before erosion can begin. The coordinate system used in this derivation is shown in Figure A1.

The element of soil mass and its velocity is then written as

$$\begin{aligned} \Delta m &= \sigma_c A \Delta y \cos \beta \\ v &= au/2 \end{aligned} \quad (A2)$$

where σ_c is the soil bulk mass density (c is the packing factor which is also equal to 1 minus the soil porosity), Δy is the element of erosion depth, β is the slope of the surface, u is the radial velocity of the gas, and $(a/2)$ is the effective proportion of the gas velocity imparted to the soil particle. By taking the proper limit, the partial differential equation describing the rate of erosion is finally obtained. The system of equations developed by Roberts, with some modifications made in Reference 3, is

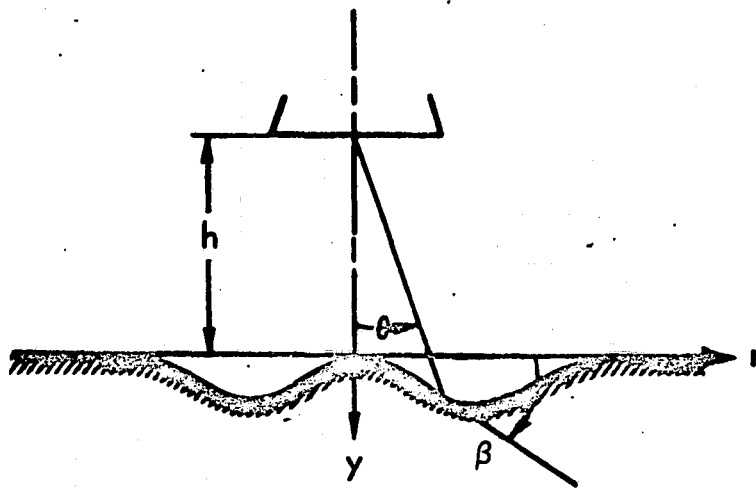


Figure A1. Coordinate System

presented following the definition of symbols. The modifications made in Reference 3 are discussed briefly following the equations.

1. Definition of Symbols

Engine Parameters

- γ = gas specific heat ratio (dimensionless)
- M_e = Mach no. at exit (dimensionless)
- r_e = nozzle exit radius (ft)
- R = gas constant ($\text{ft}^2/\text{sec}^2 \text{ } ^\circ\text{R}$)
- T_c = chamber gas temperature ($^\circ\text{R}$)
- μ_c = chamber gas viscosity ($\text{lb-sec}/\text{ft}^2$)
- p_c = chamber gas pressure (psf)
- k = engine parameter (dimensionless)

Flow Field Parameters

- p_r = recovery pressure (psf)
- p_s = stagnation pressure (psf)
- p = surface pressure (psf)
- q = dynamic pressure based on gas radial velocity u (psf)
- u = gas radial velocity along the surface (ft/sec)
- ρ = gas mass density (slugs/ft^3)
- τ = shear stress acting on soil (psf) = $q C_f$ (for rough turbulent flow)
- C_f = shear stress coefficient (dimensionless)

Soil Parameters

- a = ratio of soil particle velocity to gas velocity (dimensionless)
- D = soil particle size (ft)
- σ = soil mass density (slugs/ft^3)
- c = soil packing constant [=1 minus porosity, (dimensionless)]
- A_{coh} = cohesion parameter (Roberts recommends $5 \times 10^{-17} \text{ lb-ft}$; used 7×10^{-11} based upon $F_{coh} = 0.5 \text{ psi}$ for 30μ particle size)
- τ_{coh} = soil cohesive stress (lb/ft^2)

Soil Parameters

- α = soil internal friction angle (radians)
 τ^* = soil restraining shear stress (psf)
 v = velocity of soil particle entrained in the flow (ft/sec)

Miscellaneous Parameters

- A = cross sectional area of soil element (ft²)
 a_0, a_1 = parameter in friction coefficient equation (dimensionless)
 a_2 = parameter in h equation $\approx .25$ (dimensionless)
 a_3 = parameter in R_1 equation $\approx .5$ (dimensionless)
 C_D = particle drag coefficient (dimensionless)
 F = approximate engine thrust (lb)
 g = acceleration of gravity (ft/sec²)
 h = height of nozzle exit plane (ft)
 h_0 = nozzle height at time $t = 0$ (ft)
 h_1 = nozzle height at hover (engine cutoff) (ft)
 n = jet gas plume focusing parameter ($n=1$ in perfect vacuum, dimensionless)
 r = radial station measured from stagnation point (ft)
 R_1 = radial parameter = point at maximum viscous shear stress (ft)
 t = time (sec)
 t_1 = time at which hover/cutoff begins (sec)
 T = final time (sec)
 V_v = vertical descent rate (ft/sec)
 y = soil erosion depth (ft)
 y_{\max} = maximum value of y (along r) at each time increment (ft)
 \dot{y} = soil erosion rate (ft/sec)
 β = slope of erosion crater $\partial y / \partial r$ (radians)
 ζ = parameter in equation for " a " (dimensionless)

2. Governing Equations

Erosion Equation

$$\frac{\partial y}{\partial t} = \frac{2 (\tau - \tau^*)}{au \sigma c \cos \beta} \quad (A3)$$

Flow Field Equations

$$u = \left\{ \frac{2\gamma}{\gamma-1} RT_c \left[1 - \left(\frac{p}{p_s} \right)^{\frac{\gamma-1}{\gamma}} \right] \right\}^{\frac{1}{2}} \quad (A4)$$

$$q = \frac{\gamma}{\gamma-1} \left[1 - \left(\frac{p}{p_s} \right)^{\frac{\gamma-1}{\gamma}} \right] \left(\frac{p}{p_s} \right)^{\frac{1}{\gamma}} p_s \quad (A5)$$

$$\frac{p}{p_s} = (\cos \theta)^{n(k+4)} (\cos \beta)^2 [1 - \tan \theta \tan \beta]^2 \quad (A6)$$

$$\rho = \frac{2q}{u} \quad (A7)$$

$$\tan \theta = \frac{r}{h}, \quad \tan \beta = \frac{\partial y}{\partial r} \quad (A8)$$

$$p_s = \min \left\{ p_r, \frac{n(k+4)-2}{2} \left(\frac{r_e}{h} \right)^2 p_r \right\} \quad (A9)$$

$$p_r = \frac{\left[1 + \gamma M_e^2 \right] p_c}{\left[1 + \frac{\gamma-1}{2} M_e^2 \right]^{\frac{\gamma}{\gamma-1}}} \quad (A10)$$

$$k = \gamma(\gamma-1) M_e^2 \quad (A11)$$

$$h(t) = h_1(t) + a_2 y_{\max}(t) \quad (A12)$$

$$h_1(t) = \begin{cases} h_o - V_v t & 0 \leq t \leq t_1 \\ h_o - V_v t_1 & t > t_1 \end{cases} \quad (A13)$$

Viscous Shear Stress

$$\tau = C_f q \quad (A14)$$

Limiting Shear Stress

$$\tau^* = \sigma c D g \cos \beta \tan \alpha - \sigma c D g \sin \beta + A_{coh} D^{-3} + \tau_{coh} \quad (A15)$$

Momentum Factor

$$a^{-1} = .5 + \sqrt{.25 + \zeta^{-1}} \quad (A16)$$

$$\zeta = \frac{18\mu_c h}{\sqrt{2} \sigma D^2} \sqrt{\frac{2}{(k+4)RT_c}} \left[1 + \frac{\sqrt{2}}{72e} \frac{C_D(k+4)}{2\pi h^2} \frac{DF}{\mu_c \sqrt{RT_c}} \right] \quad (A17)$$

$$F = \pi r_e^2 p_r \text{ (used only in Equation (A17))} \quad (A18)$$

Viscous Friction Coefficient

$$C_f = a_0 + a_1 \left(\frac{y_{\max} - y}{r_e} \right) \left(\frac{y_{\max} - y}{y_{\max}} \right) \left[\frac{\frac{r}{R_1}}{1 + \left(\frac{r}{R_1} \right)^2} \right] \quad (A19)$$

$$R_1 = (h_1 + a_3 y_{\max}) \sqrt{\frac{2}{2+k}} \quad (A20)$$

3. Modifications of Roberts' Theory

In Roberts' formulation of soil erosion, it is assumed the erosion depth y is small compared to the nozzle height h . Thus, no attempt is made to change the flow field as the crater develops. In most applications of this theory, the above assumption is valid. However, during soil erosion experiments the assumption is often violated, and the erosion depth may be even larger than the original nozzle height above the uneroded surface.

In Reference 3, a comparison was made of Roberts' theory with experimental measurements of erosion obtained in a vacuum environment. In some of these tests, the depth of the erosion crater was larger than the hover nozzle height. It was appropriate, therefore, to modify Roberts' formulation to account for the effective increase in nozzle height and changes in the gas flow field. Modifications were selected on physical reasoning and then empirically adjusted by comparison of theoretical predictions and experimental findings. The motivation for the proposed modifications was made as a result of the following observations.

It seemed evident that as the soil eroded and a cavity began forming, the flow field must be altered; and hence, the shear forces acting on the soil also must change. For example, consider the region in the vicinity of the crater lip. One would expect the soil particles on the crater lip to be subjected to larger erosion forces than before the crater was formed. This seems plausible because particles on the crater lip should be exposed to a larger portion of the gas flow than when they were shielded by other particles along the flat surface. Also, such particles are more likely to be impacted by other particles dislodged from the crater itself. These effects should increase the shear forces locally and cause the crater diameter to increase with time, as one observes in erosion experiments and Roberts' theory did not predict. This increased shear force is probably due to both a change in flow and associated dynamic pressure as well as a change in viscous friction coefficient C_f . It was proposed that the changing flow field could be accounted for by simply modifying the friction coefficient. Such a modification is contained in the coefficients a_1 and a_3 in Equations (A19) and (A20). Setting these two coefficients equal to zero reduces these equations to Roberts' formulation. This modification tends to increase the friction coefficient in the vicinity of the crater lip.

Because of the weighting factor r/R_1 , the increase is larger for the outer crater lip than for the inner crater lip. It was found that the values $a_1 = 11$ and $a_3 = .5$ caused the outer crater lip radius to increase with time at a rate similar to that observed during the erosion experiments. The nozzle height h (Equation (A12)) was also modified to allow for an effective increase in nozzle height because of the development of the erosion crater. The empirically determined value for a_2 was about .25. Setting a_2 equal to zero reduces the nozzle height equation to that given by Roberts.

It is obvious that when erosion is small, the preceding modifications become negligible. In the soil erosion calculations performed in this study, the erosion was so small that the modifications were completely negligible.

Another modification is incorporated in the above set of equations through the parameter n in surface pressure Equations (A6) and (A9). Roberts' formulation corresponds to n equal to 1. The parameter n is introduced in an attempt to account for the focusing of the jet when it expands into an atmosphere. When n is larger than unity, both the stagnation pressure p_s and the rate of decay of the pressure along the surface are increased. However, for any value of n , the integrated pressure force on the entire surface is the same.

4. FORTTRAN IV Soil Erosion Program

The soil erosion program is called EROS and is written in FORTRAN IV, version 12. It is written to run on an IBM 7094 32K core machine. The program consists of a main program EROS, and five subroutines: AUXSUB, DERIV, SMOOTH, RKAN, and OUTPUT. Below is a brief description of each program.

EROS reads the Input by Namelist name "DATA." EROS saves the first three Runge Kutta integration results. When a successful Adams Moulton integration has been completed, EROS will output those time stations and radial stations specified by the user. After each integration, EROS re-evaluates the upper and lower error bounds (EV and EL) used by RKAM.

AUXSUB calculates the derivative at each radial station. This derivative is then integrated by RKAM to give the depth of the crater (ERODEP) at each radial station.

DERIV calculates the derivative at each radial station of ERODEP vs. RAD (depth vs. radius); the derivative is BETA.

SMOOTH smoothes the beta curve. The curve is smoothed NUMSMT times; if NUMSMT is not input, it is set to 2. (This feature was incorporated because it was found that small irregularities in the erosion crater tended to grow with time as a result of the differentiations to obtain the slope $\beta = \partial y / \partial r$. If uncorrected, these irregularities could lead to numerical instabilities.)

RKAM is a standard TRW subroutine which performs Runge Kutta and Adams Moulton integration. It is used to integrate ERORAT to get ERODEP.

OUTPUT. Since the output from the program can be voluminous, the user may input two quantities, DELMAX and NORAD, to control printed output. The program will write output only at time points which are a multiple of DELMAX. At each output time, every NORADth radial station will be written starting with radial station number one. The output subroutine is used to extrapolate the data, calculated for the present time, to the time point required for output. OUTPUT is called by AUXSUB only if the next time point (TIM+TIMDEL) will lie beyond the next output time. Note that the extrapolated values are used only for OUTPUT and not for calculation.

INPUT

The input is by Namelist name DATA. The following parameters must be input.

| <u>FORTTRAN</u> | <u>SYMBOL</u> | <u>DEFINITION</u> |
|-----------------|---------------|---|
| GAME | γ | Gas specific heat ratio |
| AMACH | M_e | Mach number at exit |
| GASCON | R | Gas constant ($\text{ft}^2/\text{sec}^2 \text{ } ^\circ\text{R}$) |
| RADEX | r_e | Exit radius (ft) |
| GASTEM | T_c | Chamber gas temperature ($^\circ\text{R}$) |
| GASVIS | μ_c | Chamber gas viscosity ($\text{lb-sec}/\text{ft}^2$) |
| PINF | P_o | Ambient pressure (lb/ft^2) |
| AN | n | Focusing parameter (=1 for lunar environment) |
| PARSIZ | D | Soil particle size (ft) |
| DRAGCO | C_D | Particle drag coefficient |
| SODEN | σ | Soil mass density (slugs/ft^3) |
| COHSTR | τ_{coh} | Soil cohesive stress (lb/ft^2) |
| COHPAR | A_{coh} | Cohesion parameter (lb ft) |
| ALPHA | α | Soil internal friction angle (radians) |
| A0 | a_0 | Coefficients in friction coefficient equation |
| A1 | a_1 | |
| SOPAC | c | Soil packing constant (=1 minus porosity) |
| GRAV | g | Acceleration of gravity (ft/sec^2) |
| PRES | P_c | Chamber pressure (psf) |
| HO | h_0 | Initial height of nozzle (ft) |
| HHOVER | h_1 | Hover (engine cutoff) height (ft) |
| HOVTIM | t_1 | Time at which hover/cutoff begins (sec) |
| FINTIM | T | Final time (sec) |
| VEL | V_V | Descent velocity (ft/sec) |
| A2 | a_2 | Input non-dimensional parameter in R_1 (equation) |
| A3 | a_3 | Input non-dimensional parameter in $h(t)$ (equation) |
| EPS | ϵ | Distance to first radial station (must be greater than zero because of the singularity at $r = 0$, ft) |

| <u>FORTRAN</u> | <u>SYMBOL</u> | <u>DEFINITION</u> |
|----------------|---------------|--|
| NUMRAD | | Number of radial stations |
| NUMSMT | | Number of times beta curve is smooth |
| DELMIN | | Minimum time increment (sec) |
| DELMAX | | Maximum time increment also step size for controlling output (sec) |
| RADIUS | | Radius to last radial station (ft) |
| DELTIM | | Initial time increment ($DELMIN \leq DELTIM \leq DELMAX$) |
| NORAD | | Increment for writing out selective radial stations. (Integer). 1st radial station and every NORADth station thereafter is written |
| ERRUP | | Reciprocal of % of depth for upper error bound |
| ERRLO | | Reciprocal of % of depth for lower error bound, $DELMIN \leq DELMAX$ |

OPERATING PROCEDURE

The program will accept stacked cases.

The following parameters must be considered when evaluating running time for the program: ERRUP, ERRLO, DELMIN, DELMAX, NORAD, and FINTIM. Unfortunately the first four also control the accuracy of the results.

The looser the error bounds, the faster the program runs. On test cases, $\text{ERRUP} \leq 25$ changed the results significantly.

A reasonable upper bound on the run time is 120 times FINTIM where FINTIM is in seconds.

Concerning errors, it seems best on the first run to set $\text{ERRUP} = 50$; and if the results seem unreasonable, increase ERRUP.

To have reasonable error control, the following inequalities should hold:

$$\text{ERRUP} \leq 50$$

$$\text{ERRLO} \geq 32 \text{ ERRUP}$$

Note that ERRUP is used to compute the upper bound of allowable error at each integration. It is not an upper bound for the cumulative error.

The program listing follows:

EROS

11/11/67

```
EXTERNAL AUXSUB
DIMENSION TEMP(150),TEMP1(150)
DOUBLE PRECISION TIM,TIMDEL,HOLD1
COMMON/OUTPUT/DEPTH(150,3),RATE(150,3),TIME(3),UU(150,3),
1SURF(150,3),DYNAM(150,3),RHOD(150,3),HEIGHT(3),AAA(3),
2STAG(3),PTOT(150,3),
3TFMPS(9,150),EU(150),EL(150),AUU(150,3),BETAA(150,3)
COMMON/PARAM/THET(150),BETA(150),PRESUR(150),
1DYPRES(150),U(150),RHO(150),FRICCO(150),TAU(150),TAUSTR(150),
2ERORAT(150),RAD(150),ERODEP(150),AA,GAMA,AMACH,GASCON,GAM1,
3RACCY,GASTEM,GASVIS,PINF,AN,PARSIZ,DRAGCO,SODEN,
4COHSTR,COHPAR,ALPHA,AC,A1,SOPAC,GRAV,PRES,H0,HHOVER,
5HOVTIM,FINTIM,VEL,A2,A3,EPS,NUMRAD,NUMSMT,REPRES,
6ENGPARG,F,YMAX,L,STAGPR,H,TIM,HI
NAMELIST/ DATA/GAMA,AMACH,GASCON,RADEX,GASTEM,GASVIS,
1PINF,AN,PARSIZ,DRAGCO,SODEN,COHSTR,COHPAR,ALPHA,AD,
2A1,SOPAC,GRAV,PRES,H0,HHOVER,HOVTIM,FINTIM,VEL,A2,
3A3,FPS,NUMRAD,NUMSMT,DELMIN,DELMAX,RADIUS,DELTIM,NUKAD,
4FRRUP,FRRLD
```

DATA PI/3.14159267

DATA FRRUP,FRRLD/100.,200./

1 READ (2,DATA)

C***** INITIALIZE ARRAYS

TIMDEL=DELTIM

IF (TIMDEL.LE.0.) GO TO 400

A=NUMRAD

IF (NORAD.LT.1) NORAD=1

IF (NUMSMT.LT.1) NUMSMT=2

DO 5 I=1,NUMRAD

ERORAT(I)=0.

ERODEP(I)=0.

TEMPS(1,I)=0.

FU(I)=.05

FL(I)=.05

R1=I-1

RAD(I)=R1*RADIUS/A

00000010

00000030

00000040

00000050

00000060

00000070

00000080

00000090

00000100

00000110

00000120

00000130

00000140

00000150

00000160

00000170

00000180

00000190

00000200

00000210

00000220

00000230

00000240

00000250

00000260

00000270

00000280

00000290

00000300

00000310

00000320

00000330

00000340

00000350

00000360

1

2

3

6

7

10

13

14

15

16

17

18

19

20

EROS

11/11/67

```

5  CONTINUE
   GAM1=(GAMA-1.)/GAMA
   B2=AMACH*AMACH
   R1=(1.+(GAMA-1.)/2.*B2)**(1./GAM1)
   REPRES=(1.+GAMA*B2)*PRES/B1
   ENGPAS=GAMA*(GAMA-1.)*B2
   F=PI*RADEX*RADEX*REPRES
   RAD(1)=EPS
   IFLG=-1
   IFLG2=0
   TIM=0.
   YMAX=0.
   HOLD1=DELMAX
10  ICNT=0
11  CALL RKAM (TIM,TIMDEL,ERODEP,ERORAT,AUXSUB,
   INUMRAD,0.EU,EL,DELMAX,DELMIN,ICNT,TEMPS,NH)
   IF (ICNT.LE.3.AND.IFLG.NE.1) GO TO 15
   IF (IFLG.EQ.-1) IFLG=0
   GO TO 200
C*****  SAVE FIRST THREE RUNGE KUTTA RESULTS
C*****  UNTIL WE HAVE A SUCCESSFUL ADAMS MOULTON RESULT
15  L=ICNT
   TIME(L)=TIM
   HEIGHT(L)=H1
   AAA(L)=AA
   STAG(L)=STAGPR/144.
   DO 20 I=1,NUMRAD
   DEPTH(I,L)=ERODEP(I)
   RATE(I,L)=ERORAT(I)
   UU(I,L)=U(I)
   RHOO(I,L)=RHO(I)
   AUU(I,L)=AA*U(I)
   RFTAA(I,L)=BETA(I)*57.29577
   DYNAM(I,L)=DYPRES(I)/144.
   SURF(I,L)=PRESUR(I)*STAGPR/144.
   PTOT(I,L)=SURF(I,L)+PINF/144.
20  CONTINUE

```

| | |
|----------|----|
| 00000370 | 21 |
| 00000380 | 23 |
| 00000390 | 24 |
| 00000400 | 25 |
| 00000410 | 26 |
| 00000420 | 27 |
| 00000430 | 28 |
| 00000440 | 29 |
| 00000450 | 30 |
| | 31 |
| 00000460 | 32 |
| 00000470 | 33 |
| 00000480 | 34 |
| 00000500 | 35 |
| 00000510 | |
| 00000520 | 36 |
| 00000530 | 37 |
| 00000540 | 40 |
| 00000550 | |
| 00000560 | |
| 00000570 | 43 |
| 00000580 | 44 |
| 00000590 | 45 |
| 00000600 | 46 |
| 00000610 | 47 |
| | 48 |
| 00000630 | 49 |
| 00000640 | 50 |
| 00000650 | 51 |
| 00000660 | 52 |
| 00000670 | 53 |
| 00000680 | 54 |
| 00000690 | 55 |
| 00000700 | 56 |
| 00000710 | 57 |
| 00000720 | 58 |
| 00000730 | 59 |

EROS

11/11/67

| | | | |
|--------|--|----------|-----|
| 200 | IF (IFLG)305,240,250 | 00000740 | |
| C***** | WRITE ALL THE SAVED VALUES | 00000750 | 61 |
| 240 | R1=REPRES/144. | 00000760 | 62 |
| | WRITE (3,700) ENGPAB1 | 00000770 | 63 |
| | DO 245 I=1,3 | 00000780 | 66 |
| | IFLG1=0 | | 67 |
| | IF (L.FQ.1.OR.TIME(L).EQ.HOLD1) GO TO 242 | 00000800 | 68 |
| | IF (TIME(L)+TIMDEL.LE.HOLD1) GO TO 245 | | 71 |
| | DO 230 I=1,NUMRAD | 00000830 | 74 |
| | TEMP1(I)=FRORAT(I) | | 75 |
| 230 | TEMP(I)=ERODEP(I) | 00000840 | 76 |
| | IFLG1=1 | | 78 |
| | CALL OUT (DEPTH(I,L),L,HOLD1,1,TIMDEL,TEMP1) | | 79 |
| 242 | IF (HEIGHT(L).GT.HHOVER) WRITE (3,701) | 00000860 | 80 |
| | IF (L.NE.1) HOLD1=HOLD1+DELMAX | 00000870 | 84 |
| 243 | IF (HEIGHT(L).LE.HHOVER) WRITE (3,702) | 00000880 | 87 |
| | WRITE (3,703) HEIGHT(L),TIME(L),AAA(L),STAG(L) | 00000890 | 91 |
| | WRITE (3,704) | 00000900 | 94 |
| | DO 244 I=1,NUMRAD,NUMRAD | 00000910 | 96 |
| 244 | WRITE (3,705) RAD(I),DEPTH(I,L),BETAA(I,L),RATE(I,L), | 00000920 | |
| | 1SURF(I,L),DYNAM(I,L),RHOO(I,L),AUU(I,L),UU(I,L),PTOT(I,L) | 00000930 | 97 |
| | IF (IFLG1.EQ.0) GO TO 245 | | 101 |
| | DO 235 I=1,NUMRAD | 00000940 | 104 |
| | ERORAT(I)=TEMP1(I) | | 105 |
| 235 | FRODEP(I)=TEMP(I) | 00000950 | 106 |
| 245 | CONTINUE | 00000960 | 108 |
| | IFLG=1 | 00000970 | |
| C***** | WRITE CURRENT VALUE | 00000980 | 110 |
| 250 | CONTINUE | 00000990 | 111 |
| | IFLG1=0 | 00001000 | 112 |
| | TTIM=TIM | 00001020 | 113 |
| | IF (TIM.FQ.HOLD1) GO TO 252 | 00001040 | 114 |
| | IF (IFLG2.EQ.1) GO TO 221 | | 117 |
| | IF (TIM+TIMDEL.LE.HOVTIM) GO TO 221 | | 120 |
| | IFLG2=1 | | 123 |
| | HOLD2=HOVTIM | | 124 |
| | DO 215 I=1,NUMRAD | | 125 |

EROS

11/11/67

| | | | |
|--------|---|----------|-----|
| | TEMP1(I)=ERORAT(I) | | 126 |
| 215 | TEMP(I)=ERODEP(I) | | 127 |
| | IFLG1=1 | | 129 |
| | CALL OUT (ERODEP.L.HOLD2.2.TIMDEL,TEMP1) | | 130 |
| | WRITE (3.702) | | 131 |
| | TTIM=HOVTIM | | 133 |
| | IF (HOVTIM.EQ.HOLD1) HOLD1=HOLD1+DELMAX | | 134 |
| | GO TO 216 | | 137 |
| 221 | IF (TIM+TIMDEL.LE.HOLD1) GO TO 255 | | 138 |
| | DO 220 I=1.NUMRAD | 00001060 | 141 |
| | TEMP1(I)=ERORAT(I) | | 142 |
| 220 | TEMP(I)=ERODEP(I) | 00001070 | 143 |
| | IFLG1=1 | 00001080 | 145 |
| | CALL OUT (ERODEP.L.HOLD1.2.TIMDEL,TEMP1) | | 146 |
| 252 | IF (HOLD1.LT.HOVTIM) WRITE (3.701) | | 147 |
| | TTIM=HOLD1 | 00001110 | 151 |
| 253 | IF (HOLD1.GE.HOVTIM) WRITE (3.702) | | 152 |
| | HOLD1=HOLD1+DELMAX | 00001120 | 156 |
| 216 | CONTINUE | | 157 |
| | B3=STAGPR/144. | | 158 |
| | WRITE (3.703) HI.TTIM.AA.B3 | | 159 |
| | WRITE (3.704) | 00001150 | 162 |
| | DO 254 I=1.NUMRAD.NORAD | 00001160 | 164 |
| | B1=BETA(I)*57.29577 | 00001170 | 165 |
| | B2=AA*U(I) | 00001180 | 166 |
| | B3=PRESUR(I)*STAGPR/144. | 00001190 | 167 |
| | B4= B3+PINF/144. | 00001200 | 168 |
| | B5=DYPRES(I)/144. | 00001210 | 169 |
| | WRITE (3.705) RAD(I).ERODEP(I).B1.ERGRAT(I).B3. B5. | 00001220 | |
| | IRHO(I).B2.U(I).B4 | 00001230 | 170 |
| 254 | CONTINUE | 00001240 | 173 |
| | IF (IFLG1.EQ.0) GO TO 255 | 00001250 | 175 |
| | DO 225 I=1.NUMRAD | 00001260 | 178 |
| | ERORAT(I)=TEMP1(I) | | 179 |
| 225 | ERODEP(I)=TEMP(I) | 00001270 | 180 |
| 255 | CONTINUE | 00001280 | |
| C***** | SET NEW ERROR BOUNDS FOR RKAM | 00001290 | 182 |

EROS

11/11/67

| | | | |
|--------|---|----------|-----|
| 305 | YMAX=ERODEP(I) | 00001300 | 183 |
| | DO 310 I=1,NUMRAD | 00001310 | 184 |
| | EU(I)=ABS(ERODEP(I)/ERRUP) | 00001320 | 185 |
| | EL(I)=ABS(ERODEP(I)/ERRLO) | 00001330 | 186 |
| | YMAX=AMAX1(YMAX,ERODEP(I)) | 00001340 | 187 |
| 310 | CONTINUE | 00001350 | |
| C***** | IF NECESSARY ADJUST TIME INCREMENT ON | 00001360 | |
| C***** | LAST PASS | 00001370 | 188 |
| | IF (TIM.GE.FINTIM) GO TO 1 | 00001380 | 190 |
| | IF (FINTIM-TIM-TIMDEL) 320,11,11 | 00001390 | 193 |
| 320 | TIMDEL=FINTIM-TIM | 00001400 | 194 |
| | GO TO 10 | 00001410 | 195 |
| 400 | WRITE (3,706) | 00001420 | 196 |
| | GO TO 1 | 00001430 | 198 |
| 700 | FORMAT (35H | 00001440 | |
| | ENGINE PARAMETER =E15.8// | 00001450 | |
| 135H | RECOVERY PRESSURE (PSI) =E15.8///) | 00001460 | |
| 701 | FORMAT (//15H | 00001470 | |
| | DESCENDING//) | 00001480 | |
| 702 | FORMAT (//13H | 00001490 | |
| | HOVERING//) | 00001500 | |
| 703 | FORMAT (30H | 00001510 | |
| | NOZZLE HEIGHT (FT) =E15.8,21X, | 00001520 | |
| | 16H TIME =F10.4//30H | 00001530 | |
| | MOMENTUM FACTOR A =E15.8, | 00001540 | |
| | 210X.27H STAGNATION PRESSURE (PSI) =E15.8) | 00001550 | |
| 704 | FORMAT (///51X.5HSURF..8X.4HDYN..20X.5HPART..7X.3HGAS.9X.5HTOTAL/ | 00001560 | |
| 1 | 12H STATION 12H DEPTH 12H SLOPE 12H RATE | 00001570 | |
| 2 | 12H PRESS. 12H PRESS. 12H GAS DENS. 12H VEL. | 00001580 | |
| 3 | 12H VFL. 12H PRESS. /12H (FT) 12H (FT) | 00001590 | |
| 4 | 12H (DEG) 12H (FT/SEC) 12H (PSI) 12H (PSI) | 00001600 | |
| 5 | 12H SLUG/CU FT 12H (FT/SEC) 12H (FT/SEC) 12H (PSI) /// | | |
| 705 | FORMAT (10(1X.E11.4)) | | |
| 706 | FORMAT (61H NO TIME INCREMENT (DELTIM) FOR CASE. I'M GOING TO NEX | | |
| | IT CASE) | | |
| | END | | |

AUXSUB

10/26/67

SUBROUTINE AUXSUB (ICNT)
 DOUBLE PRECISION TIM,TIMDEL
 COMMON/PARAM/THET(150),BETA(150),PRESUR(150),
 10YPRES(150),U(150),RHO(150),FRICCO(150),TAU(150),TAUSTR(150),
 2ERORAT(150),RAD(150),ERODEP(150),AA,GAMA,AMACH,GASCON,GAM1,
 3RADEX,GASTEM,GASVIS,PINF,AN,PARSIZ,DRAGCO,SDDEN,
 4COHSTR,COHPAR,ALPHA,AC,A1,SOPAC,GRAV,PRES,H0,HHOVER,
 5HOVTIM,FINTIM,VEL,A2,A3,EPS,NUMRAD,NUMSMT,REPRES,
 6ENGPARG,F,YMAX,L,STAGPR,H,TIM,H1

DATA PI/3.1415926/

IF (ICNT.NE.1) GO TO 5

IF (L.NE.1) YMAX=0.

5 CONTINUE

C***** CALCULATE PARAMETERS THAT ARE CONSTANT WITH

C***** RESPECT TO RADIUS

IF (TIM-HOVTIM) 1,1,2

1 H1=HC-VEL*TIM

GO TO 3

2 H1=HC-VEL*HOVTIM

3 H=H1+A2*YMAX

R1=(H1+A3*YMAX)*SQRT(2./(2.+ENGPARG))

B1=(AN*(ENGPARG+4.)-2.)/2.*REPRES*((RADEX/4)**2)

STAGPR=AMIN1(REPRES,B1)

B1=18.*GASVIS*H/(1.414214*SDDEN*PARSIZ*PARSIZ)

B2=SQRT(2./((ENGPARG+4.)*GASCON*GASTEM))

B3=1.+1.414214/195.7162*DRAGCO*(ENGPARG+4.)/

1 (2.*PI*H*H)*PARSIZ*F/(GASVIS*SQRT(GASCON*GASTEM))

ZETA=B1*B2*B3

AA=1./(.5+SQRT(.25+1./ZETA))

C***** CALCULATE PARAMETERS AT RADIAL STATIONS

DO 20 I=1,NUMRAD

20 THET(I)=ATAN2(RAD(I),H)

C***** BETA IS SLOPE OF ERODEP VS. RAD

CALL DERIV (ERODEP,RAD,BETA,NUMRAD)

DO 30 I=1,NUMRAD

30 BETA(I)=ATAN(BETA(I))

00000010

00000020

00000030

00000040

00000050

00000060

00000070

00000080

00000090

00000100

00000110

1

00000120

4

00000130

00000140

00000150

7

00000160

8

00000170

9

00000180

10

00000190

11

00000200

12

00000210

13

00000220

14

00000230

15

00000240

16

00000250

17

00000260

00000270

18

00000280

19

00000290

00000300

20

00000310

21

00000320

00000330

22

00000340

24

00000350

25

00000360

AUXSUB

10/26/67

```

C***** SMOOTH BETA CURVE   NUMSMT = NUMBER OF TIMES
C***** CURVE IS SMOOTHED
      CALL SMOOTH (BETA,NUMRAD,NUMSMT)
C***** CALCULATE THE DERIVATIVE AT EACH RADIAL STATION
      DO 40 I=1,NUMRAD
        B1=COS(THET(I))*((AN*(ENGPAT+4.))*(COS(BETA(I))**2)
        PRESUR(I)=B1*((1.-TAN(THET(I))*TAN(BETA(I))**2)
        DYPRES(I)=1./GAM1*(1.-(PRESUR(I)**GAM1))*STASPR*
1      (PRESUR(I)**(1./GAMA))
        B1=(2./GAM1)*GASCON*GASTEN*(1.-PRESUR(I)**GAM1)
        U(I)=B1**5
        RHO(I)=2.*DYPRES(I)/(U(I)*U(I))
        B1=RAD(I)/R1
        FRICCO(I)=A0+A1*((YMAX-ERODEP(I))**2)/
1      (RADEX*YMAX)*B1/(1.+B1*B1)
        IF (YMAX.LE.C.) FRICCO(I)=A0
        TAU(I)=FRICCO(I)*DYPRES(I)
        B1=SODEN*PARSI7 *SOPAC*GRAV
        B2=COS(BETA(I))*TAN(ALPHA)-SIN(BETA(I))
        TAUSTR(I)=B1*B2+COHPAR/(PARSI2**3)+COHSTR
        IF (TAU(I)-TAUSTR(I)) 34,34,35
34      ERORAT(I)=C.
        GO TO 40
35      ERORAT(I)=2.*(TAU(I)-TAUSTR(I))/(AA*SODEN*
1      SOPAC*U(I)*COS(BETA(I)))
40      CONTINUE
      RETURN
      END

```

| | |
|----------|----|
| 00000370 | |
| 00000380 | 26 |
| 00000390 | |
| 00000400 | 28 |
| 00000410 | 29 |
| 00000420 | 30 |
| 00000430 | 31 |
| 00000440 | |
| 00000450 | 32 |
| 00000460 | 33 |
| 00000470 | 34 |
| 00000480 | 35 |
| 00000490 | 36 |
| 00000500 | |
| 00000510 | 37 |
| | 38 |
| 00000520 | 41 |
| 00000530 | 42 |
| 00000540 | 43 |
| 00000550 | 44 |
| 00000560 | 45 |
| 00000570 | 46 |
| 00000580 | 47 |
| 00000590 | |
| 00000600 | 48 |
| 00000610 | 49 |
| 00000620 | 51 |
| 00000630 | 52 |

DERIV

10/09/67

```

SUBROUTINE DERIV (Y,RAD,BETA,N)
C*****  BETA IS SLOPE OF Y VS. RAD
DIMENSION Y(N),RAD(N),BETA(N)
C*****  N MUST BE GREATER THAN OR EQUAL TO 5
IF (N.LT.5) GO TO 100
H=12.*(RAD(2)-RAD(1))
BETA(1)=(-25.*Y(1)+48.*Y(2)-36.*Y(3)+16.*Y(4)-3.*Y(5))/H
H=12.*(RAD(3)-RAD(2))
BETA(2)=(-3.*Y(1)-10.*Y(2)+18.*Y(3)-6.*Y(4)+Y(5))/H
NNK=N-2
CC 1 I=3,NNK
1  BETA(I)=(Y(I-2)-8.*Y(I-1)+8.*Y(I+1)-Y(I+2))/H
  BETA(N-1)=(-Y(N-4)+6.*Y(N-3)-18.*Y(N-2)+10.*Y(N-1)+3.*Y(N))/H
  BETA(N)=(3.*Y(N-4)-16.*Y(N-3)+36.*Y(N-2)-48.*Y(N-1)
1    +25.*Y(N))/H
  RETURN
100 WRITE (3,101)
101 FORMAT (37H IN SUBROUTINE DERIV N IS LESS THAN 5)
  RETURN
  END

```

1
4
5
6
7
8
9
10
12
13
14
15
17
18

SMOOTH

10/24/67

SUBROUTINE SMOOTH (BETA,N,NN)

DIMENSION BETA(N),R(150)

IF (N.LT.5) GO TO 100

DO 2 JJ=1,NN

$$R(1) = (69.*BETA(1) + 4.*BETA(2) - 6.*BETA(3) + 4.*BETA(4) - BETA(5)) / 70.$$

$$R(2) = (2.*BETA(1) + 27.*BETA(2) + 12.*BETA(3) - 8.*BETA(4) + 2.*BETA(5)) / 35.$$

NNK=N-2

DO 1 I=3,NNK

$$R(I) = (-3.*BETA(I-2) + 12.*BETA(I-1) + 17.*BETA(I) + 12.*BETA(I+1) - 3.*BETA(I+2)) / 35.$$

$$R(N-1) = (2.*BETA(N) + 27.*BETA(N-1) + 12.*BETA(N-2) - 8.*BETA(N-3) + 2.*BETA(N-4)) / 35.$$

$$R(N) = (69.*BETA(N) + 4.*BETA(N-1) - 6.*BETA(N-2) + 4.*BETA(N-3) - BETA(N-4)) / 70.$$

DO 3 I=1,N

BETA(I)=R(I)

CONTINUE

RETURN

100 WRITE (3,101)

101 FORMAT (38H IN SUBROUTINE SMOOTH N IS LESS THAN 5)

RETURN

END

1
4
5
6
7
8
9
11
12
13
14
16
18
19
21
22

RKAM

10/04/67

```

SUBROUTINE RKAM(XDP,HDP,VAR,DER,AUXSUB,N,OPT,
!FU,EL,HMAX,HMIN,ICNT,TEMPS,NH)
DOUBLE PRECISION XDP,HDP,CDP
DIMENSION VAR(1),DEP(1),FU(1),EL(1),TEMPS(9,1),C(2)
EQUIVALENCE (CDP,C)
NN=N
C EXIT IF N IS ZERO OR NEGATIVE
  IF(NN.LE.0) RETURN
  IC=ICNT
C TRANSFER ON R-K ONLY OPTION
  IF(OPT.NE.0.0) GO TO 200
  IF(IC.GT.2) GO TO 110
C COUNTER IS LESS THAN 3--RUNGA-KUTTA STEP
  K=1
  IC=IC+1
  IF(IC.GT.1) GO TO 120
C COUNTER WAS ZERO ON ENTRY--STORE INITIAL ORDINATES
100 DO 105 I=1,NN
    TEMPS(5,I)=TEMPS(1,I)
105 TEMPS(6,I)=VAR(I)
  GO TO 120
C COUNTER IS GREATER THAN 2--ADAMS-MOULTON STEP
C STORE ENTRY ORDINATES
110 DO 115 I=1,NN
    TEMPS(2,I)=VAR(I)
115 TEMPS(3,I)=TEMPS(1,I)
  K=0
C STORE ENTRY DERIVATIVES
120 DO 125 I=1,NN
125 TEMPS(4,I)=DER(I)
  IF(K.EQ.0) GO TO 300
C INTEGRATE ONE STEP WITH P-K
200 K=0
  DO 205 I=1,NN
    TEMPS(2,I)=VAR(I)
205 TEMPS(3,I)=DER(I)

```

```

RKAM0002
RKAM0003
RKAM0004
RKAM0005
RKAM0006
RKAM0007
RKAM0008 1
RKAM0009 2
RKAM0010
RKAM0011 5
RKAM0012 6
RKAM0013
RKAM0014 9
RKAM0015 12
RKAM0016 13
RKAM0017
RKAM0018 14
RKAM0019 17
RKAM0020 18
RKAM0021 19
RKAM0022
RKAM0023
RKAM0024 21
RKAM0025 22
RKAM0026 23
RKAM0027 24
RKAM0028
RKAM0029 26
RKAM0030 27
RKAM0031 28
RKAM0032
RKAM0033 30
RKAM0034 33
RKAM0035 34
RKAM0036 35
RKAM0037 36

```

PKAM

10/04/67

```

      CDP=HDP/2.00
      A=C(1)
210  XDP=XDP+CDP
215  DO 220 I=1,NN
220  VAR(I)=TEMPS(2,I)+A*DER(I)
      CALL AUXSUB (IC)
      K=K+1
      IF(K.EQ.3) GO TO 230
      DO 225 I=1,NN
225  TEMPS(3,I)=TEMPS(3,I)+2.0*DER(I)
      IF(K.EQ.1) GO TO 215
      A=HDP
      GO TO 210
230  A=A/6.0
      DO 235 I=1,NN
      C(1)=TEMPS(2,I)
      C(2)=TEMPS(1,I)
      R=(TEMPS(3,I)+DER(I))*A
      CDP=CDP+R
      VAR(I)=C(1)
235  TEMPS(1,I)=C(2)
      CALL AUXSUB (IC)
      IF(OUT.NE.0.0) RETURN
      GO TO 600
C    INTEGRATE ONE STEP WITH A-M AND TEST STEP SIZE
300  A=HDP/24.0
      XDP=XDP+HDP
      DO 310 I=1,NN
      TEMPS(1,I)=A*(55.0*TEMPS(4,I)-59.0*TEMPS(5,I)
1+37.0*TEMPS(6,I)-0.0*TEMPS(7,I))
      C(1)=TEMPS(2,I)
      C(2)=TEMPS(3,I)
310  VAR(I)=CDP+TEMPS(1,I)
      CALL AUXSUB (IC)
      K=0
      DO 325 I=1,NN
      R=A*(0.0*DER(I)+10.0*TEMPS(4,I)-5.0*TEMPS(5,I)+TEMPS(6,I))

```

| | |
|----------|----|
| RKAM0038 | 38 |
| RKAM0039 | 39 |
| RKAM0040 | 40 |
| RKAM0041 | 41 |
| RKAM0042 | 42 |
| | 44 |
| RKAM0044 | 45 |
| RKAM0045 | 46 |
| RKAM0046 | 49 |
| RKAM0047 | 50 |
| RKAM0048 | 52 |
| RKAM0049 | 55 |
| RKAM0050 | 56 |
| RKAM0051 | 57 |
| RKAM0052 | 58 |
| RKAM0053 | 59 |
| RKAM0054 | 60 |
| RKAM0055 | 61 |
| RKAM0056 | 62 |
| RKAM0057 | 63 |
| RKAM0058 | 64 |
| | 66 |
| RKAM0060 | 67 |
| RKAM0061 | |
| RKAM0062 | 70 |
| RKAM0063 | 71 |
| RKAM0064 | 72 |
| RKAM0065 | 73 |
| RKAM0066 | |
| RKAM0067 | 74 |
| RKAM0068 | 75 |
| RKAM0069 | 76 |
| RKAM0070 | 77 |
| | 79 |
| RKAM0072 | 80 |
| RKAM0073 | 81 |
| RKAM0074 | 82 |

RKAM

10/24/67

```

C=ARC(R-TEMPS(1,I))
IF(C.LT.FL(I)) GO TO 320
K=1
IF(C.LT.FU(I)) GO TO 320
IF(ABS(HDP).GT.(2.*HMIN)) GO TO 500
320 C(1)=TEMPS(2,I)
C(2)=TEMPS(3,I)
CDP=CDP+R
VAR(1)=C(1)
325 TEMPS(1,I)=C(2)
CALL AUXSUB (IC)
IF(IC.GT.3) GO TO 330
IC=4
330 IF(K.EQ.0) GO TO 340
IC=4
GO TO 600
340 IC=IC+1
IF(IC.LT.7) GO TO 600
IF(ABS(HDP).GT.(HMAX/2.0)) GO TO 600
C DOUBLING PROCESS--REARRANGE DERIVATIVES AND EXIT
400 IC=4
HDP=HDP*2.000
DO 410 I=1,NN
TEMPS(6,I)=TEMPS(7,I)
410 TEMPS(7,I)=TEMPS(9,I)
GO TO 700
C HALVING PROCESS
C COUNTER L.T. 4--BACK 3 STEPS--RESTART R-K WITH H/2
C COUNTER G.T. 3--INTERPOLATE--REDO LAST STEP WITH H/2
500 CDP=HDP
NH=I
HDP=HDP/2.000
IF(IC.GE.4) GO TO 520
IC=1
XDP=XDP-4.000*CDP
DO 510 I=1,NN
VAR(I)=TEMPS(9,I)

```

| | |
|----------|-----|
| RKAM0075 | 83 |
| RKAM0076 | 84 |
| RKAM0077 | 87 |
| RKAM0078 | 88 |
| RKAM0079 | 91 |
| RKAM0080 | 94 |
| RKAM0081 | 95 |
| RKAM0082 | 96 |
| RKAM0083 | 97 |
| RKAM0084 | 98 |
| | 100 |
| RKAM0086 | 101 |
| RKAM0087 | 104 |
| RKAM0088 | 105 |
| RKAM0089 | 108 |
| RKAM0090 | 109 |
| RKAM0091 | 110 |
| RKAM0092 | 111 |
| RKAM0093 | |
| RKAM0094 | 114 |
| RKAM0095 | 117 |
| RKAM0096 | 118 |
| RKAM0097 | 119 |
| RKAM0098 | 120 |
| RKAM0099 | 121 |
| RKAM0100 | |
| RKAM0101 | |
| RKAM0102 | |
| RKAM0103 | 123 |
| RKAM0104 | 124 |
| RKAM0105 | 125 |
| RKAM0106 | 126 |
| RKAM0107 | 127 |
| RKAM0108 | 130 |
| RKAM0109 | 131 |
| RKAM0110 | 132 |
| RKAM0111 | 133 |

OKAM

10/04/67

| | | | |
|-----|--|----------|-----|
| | TEMPS(1,1)=TEMPS(8,1) | RKAM0112 | 134 |
| 510 | DER(1)=TEMPS(7,1) | RKAM0113 | 135 |
| | GO TO 100 | RKAM0114 | 137 |
| 520 | XDP=XDP-CDP | RKAM0115 | 138 |
| | IC=4 | RKAM0116 | 139 |
| | DO 530 I=1,NN | RKAM0117 | 140 |
| | A=(5.*(TEMPS(4,1)+2.*(TEMPS(5,1)-TEMPS(6,1))+TEMPS(7,1))/16.0 | RKAM0118 | 141 |
| | TEMPS(7,1)=(9.*(TEMPS(5,1)+TEMPS(6,1))-TEMPS(4,1)-TEMPS(7,1))/16.0 | RKAM0119 | 142 |
| | TEMPS(6,1)=TEMPS(5,1) | RKAM0120 | 143 |
| 530 | TEMPS(5,1)=A | RKAM0121 | 144 |
| | GO TO 300 | RKAM0122 | |
| | MOVE PAST DATA | RKAM0123 | 146 |
| 600 | DO 610 J=1,5 | RKAM0124 | 147 |
| | K=10-J | RKAM0125 | 148 |
| | DO 610 I=1,NN | RKAM0126 | 149 |
| 610 | TEMPS(K,I)=TEMPS(K-1,I) | RKAM0127 | 150 |
| 700 | ICNT=IC | RKAM0128 | 153 |
| 705 | RETURN | RKAM0129 | 154 |
| | END | RKAM0130 | 155 |

OUT

11/09/67

```
SUBROUTINE OUT (HOLE,L,HOLD1,NBRAN,TIMDEL,TEMP1)
  DIMENSION HOLE(1),B(4),TEMP1(1)
  DOUBLE PRECISION TIM,TIMDEL,HOLD1,TTIM
  COMMON/OUTPUT/DEPTH(150,3),RATE(150,3),TIME(3),UU(150,3),
  1SURF(150,3),DYNAM(150,3),RHOO(150,3),HEIGHT(3),AAA(3),
  2STAG(3),PTOT(150,3),
  3TEMPS(9,150),EU(150),EL(150),AUU(150,3),BETAA(150,3)
  COMMON/PARAM/THET(150),BETA(150),PRESUR(150),
  1DYPRES(150),U(150),RHO(150),FRICCO(150),TAU(150),TAUSTR(150),
  2ERORAT(150),RAD(150),ERODEP(150),AA,GAMA,AMACH,GASCON,GAM1,
  3BRADEX,GASTEM,GASVIS,PINF,AN,PARSIZ,DRAGCO,SODEN,
  4COHSTR,COHPAR,ALPHA,AO,A1,SOPAC,GRAV,PRES,H0,HUOVER,
  5HOVTIM,FINTIM,VEL,A2,A3,EPS,NUMRAD,NUMSMT,REPRES,
  6ENGPARG,F,YMAX,L,STAGPR,H,TIM,H1
```

```
  IF (NBRAN.EQ.2) GO TO 10
  DO 5 I=1,NUMRAD
5   ERODEP(I)=HOLE(I)
10  CONTINUE
  YYMAX=YMAX
  YMAX=ERODEP(1)
  DO 11 I=1,NUMRAD
11  YMAX=AMAX1(ERODEP(I),YMAX)
  TTIM=TIM
  TIM=HOLD1
  CALL AUXSUB (5)
  TIM=TTIM
  YMAX=YYMAX
  S=(HOLD1-TIM)/TIMDEL
  B(1)=S*S*S+8.*S*S+22.*S+24.
  B(2)=-S*(3.*S*S+20.*S+36.)
  B(3)=S*(3.*S*S+16.*S+18.)
  B(4)=-S*(S+2.)*(S+2.)
  DO 15 I=1,NUMRAD
  SUM=TEMP1(I)
  DO 12 J=2,4
12  SUM=SUM+B(J)*TEMPS(J+3,I)
```

| | |
|----------|----|
| 00000030 | |
| 00000040 | |
| 00000050 | |
| 00000060 | |
| 00000070 | |
| 00000080 | |
| 00000090 | |
| 00000100 | |
| 00000110 | |
| 00000120 | |
| 00000130 | |
| 00000140 | |
| 00000150 | 1 |
| 00000160 | 4 |
| 00000170 | 5 |
| 00000180 | 7 |
| 00000190 | 8 |
| 00000200 | 9 |
| 00000210 | 10 |
| 00000220 | 11 |
| 00000230 | 13 |
| 00000240 | 14 |
| 00000250 | 15 |
| 00000260 | 16 |
| 00000270 | 17 |
| 00000280 | 18 |
| 00000290 | 19 |
| 00000300 | 20 |
| 00000310 | 21 |
| 00000320 | 22 |
| 00000330 | 23 |
| | 24 |
| | 25 |
| 00000360 | 26 |

OUT

11/09/67

```

15  ERODEP(I)=ERODEP(I)+SUM*(HOLD1-TIM)/24.
    CONTINUE
    IF (NBRAN.EQ.2) RETURN
    TIME(L)=HOLD1
    HEIGHT(L)=H1
    AAA(L)=AA
    STAG(L)=STAGPR/144.
    DO 20 I=1,NUMRAD
    DEPTH(I,L)=ERODEP(I)
    RATE(I,L)=ERORAT(I)
    UU(I,L)=U(I)
    RHOO(I,L)=RHO(I)
    AJU(I,L)=AA*U(I)
    BFTAA(I,L)=BETA(I)*57.29577
    DYNAM(I,L)=DYPRES(I)/144.
    SURF(I,L)=PRESUR(I)*STAGPR/144.
    PTOT(I,L)=SURF(I,L)+PINF/144.
20  CONTINUE
    RETURN
    END

```

```

00000370 28
00000380 29
00000390 31
00000400 34
00000410 35
00000420 36
          37
00000440 38
00000450 39
00000460 40
00000470 41
00000480 42
00000490 43
00000500 44
00000510 45
00000520 46
00000530 47
00000540 48
00000550 50
00000560 51

```

5. Example FORTRAN IV Soil Erosion Calculations

Example calculations are presented in this section for the following parameter values

| | |
|--|---|
| $\gamma = 1.252$ | $n = 1$ |
| $M_e = 3.98$ | $a_o = .2$ |
| $R = 2310 \text{ ft}^2/\text{sec}^2 \text{ } ^\circ\text{R}$ | $a_1 = 0$ |
| $r_e = .389 \text{ ft}$ | $a_2 = 0$ |
| $T_c = 5670 \text{ } ^\circ\text{R}$ | $a_3 = 0$ |
| $\mu_c = 1 \times 10^{-6} \text{ lb-sec/ft}^2$ | $c = .5$ |
| $\alpha = 34 \text{ deg } (0.593 \text{ rad})$ | $C_D = 2$ |
| $g = 12.3 \text{ ft/sec}^2$ | $A_{coh} = 0$ |
| $\sigma = 5.81 \text{ slugs/ft}^3$ | $\tau_{coh} = 0$ |
| $h_o = 40 \text{ ft}^*$ | $V_v = 5 \text{ ft/sec}$ |
| $p_o = .0726 \text{ psia } (10.45 \text{ psf})$ | $p_c = 42.5 \text{ psia } (6120 \text{ psf})$ |
| $D = 300 \text{ microns } (0.000984 \text{ ft})$ | |

The first output data sheet lists the input parameters, the computed value of k , recovery pressure p_r , and the soil erosion data at $t = 0.1 \text{ sec}$ ($h = 39.5 \text{ ft}$). The second output data sheet shows the erosion data at $t = 2 \text{ sec}$ ($h = 30 \text{ ft}$) and $t = 4 \text{ sec}$ ($h = 20 \text{ ft}$). The output data are the radial station r , erosion depth y , erosion crater slope β , erosion rate \dot{y} , surface pressure p , dynamic pressure q , gas density ρ , soil particle velocity v , gas velocity u , and total surface pressure $p + p_o$. Also shown are the momentum factor "a" and stagnation pressure p_s at the various nozzle heights.

*An initial nozzle height of 40 feet, rather than 100 feet, was used in this example, because no erosion takes place above a 40-foot nozzle height for the 300 micron particles. Observe, for example, on pages A-29 and A-30 that the erosion rate is zero at all radial stations at the 40-foot nozzle height, while soil is eroding at a 30-foot nozzle height.

SDATA

SYSTEM

GAMA=1.252, ANACH=3.58, GASCON=2310., RADEX=.389,

GASTEM=5670., GASVIS=1.E-6, PINF=10.45, AN=1,

PARSIZ=.000984, DRAGCO=2., SODEN=5.91, COHSTR=0.,

COHPAR=0., ALPHA=.523348, A0=.2, A1=0., A2=C., A3=0.,

SOPAC=.5, GRAV=12.3, PRES=6120., HO=40.,

HMOVER=15., HOVTIM=5., FINTIM=4., VEL=5.,

CPS=1., C-5, NUMRAD=12, NOPAD=1, NUMSMT=2,

RADIUS=24., DELMIN=.1, DELMAX=2., DELTIM=.1,

ERRUP=50., ERRLO=400., \$END

ENGINE PARAMETER = 0.4997292E 01

RECOVERY PRESSURE (PSI) = 0.37585849E 01

DESCENDING

NOZZLE HEIGHT (FT) = 0.39501000E 02

TIME = 0.1000

MOMENTUM FACTOR A = 0.10228068E-00

STAGNATION PRESSURE (PSI) = 0.12889994E-02

| STATION (FT) | DEPTH (FT) | SLOPE (DEG) | RATE (FT/SEC) | SURF. PRESS. (PSI) | DYN. PRESS. (PSI) | GAS DENS. SLUG/CU FT | PART. VEL. (FT/SEC) | GAS VEL. (FT/SEC) | TOTAL PRESS. (PSI) |
|-----------------|---------------|----------------|------------------|--------------------------|-------------------------|-------------------------|---------------------------|-------------------------|--------------------------|
| 0.1000E-04 | 0. | -0. | 0. | 0.1299E-02 | -0. | -0. | -0. | -0. | 0.7386E-01 |
| 0.2000E-01 | 0. | -0. | 0. | 0.1274E-02 | 0.1469E-04 | 0.1404E-07 | 0.5615E 02 | 0.5490E 03 | 0.7384E-01 |
| 0.4000E-01 | 0. | -0. | 0. | 0.1231E-02 | 0.5577E-04 | 0.1366E-07 | 0.1119E 03 | 0.1094E 04 | 0.7380E-01 |
| 0.5000E-01 | 0. | 0. | 0. | 0.1163E-02 | 0.1206E-03 | 0.1306E-07 | 0.1668E 03 | 0.1631E 04 | 0.7373E-01 |
| 0.8000E-01 | 0. | -0. | 0. | 0.1076E-02 | 0.1981E-03 | 0.1227E-07 | 0.2206E 03 | 0.2157E 04 | 0.7365E-01 |
| 0.1000E-02 | 0. | -0. | 0. | 0.9747E-03 | 0.2802E-03 | 0.1134E-07 | 0.2729E 03 | 0.2668E 04 | 0.7354E-01 |
| 0.1200E-02 | 0. | -0. | 0. | 0.9665E-03 | 0.3583E-03 | 0.1032E-07 | 0.3234E 03 | 0.3162E 04 | 0.7344E-01 |
| 0.1400E-02 | 0. | -0. | 0. | 0.7569E-03 | 0.4253E-03 | 0.9263E-08 | 0.3719E 03 | 0.3637E 04 | 0.7333E-01 |
| 0.1600E-02 | 0. | -0. | 0. | 0.6507E-03 | 0.4768E-03 | 0.8210E-08 | 0.4183E 03 | 0.4090E 04 | 0.7322E-01 |
| 0.1800E-02 | 0. | -0. | 0. | 0.5516E-03 | 0.5106E-03 | 0.7194E-08 | 0.4624E 03 | 0.4521E 04 | 0.7312E-01 |
| 0.2000E-02 | 0. | 0. | 0. | 0.4617E-03 | 0.5266E-03 | 0.6241E-08 | 0.5042E 03 | 0.4929E 04 | 0.7303E-01 |
| 0.2200E-02 | 0. | 0. | 0. | 0.3823E-03 | 0.5264E-03 | 0.5368E-08 | 0.5436E 03 | 0.5315E 04 | 0.7295E-01 |

DESCENDING

NOZZLE HEIGHT (FT) = 0.30000000E 04

TIME = 2.0000

MOMENTUM FACTOR A = 0.89785561E-01

STAGNATION PRESSURE (PSI) = 0.22346237E-02

| STATION (FT) | DEPTH (FT) | SLOPE (DEG) | RATE (FT/SEC) | SURF. PRESS. (PSI) | DYN. PRESS. (PSI) | GAS DENS. SLUG/CU FT | PART. VEL. (FT/SEC) | GAS VEL. (FT/SEC) | TOTAL PRESS. (PSI) |
|-----------------|---------------|----------------|------------------|--------------------------|-------------------------|-------------------------|---------------------------|-------------------------|--------------------------|
| 0.1000E-04 | 0. | 0.1393E-07 | 0. | 0.2235E-02 | -0. | -0. | -0. | -0. | 0.7480E-01 |
| 0.2000E 01 | 0. | -0.5573E-07 | 0. | 0.2190E-02 | 0.4379E-04 | 0.2418E-07 | 0.6484E 02 | 0.7222E 03 | 0.7476E-01 |
| 0.4000E 01 | 0. | 0.8360E-07 | 0. | 0.2064E-02 | 0.1650E-03 | 0.2306E-07 | 0.1289E 03 | 0.1435E 04 | 0.7463E-01 |
| 0.6000E 01 | 0. | -0.2374E-06 | 0. | 0.1873E-02 | 0.3365E-03 | 0.2134E-07 | 0.1913E 03 | 0.2131E 04 | 0.7444E-01 |
| 0.8000E 01 | 0. | -0.6967E-06 | 0. | 0.1641E-02 | 0.5231E-03 | 0.1913E-07 | 0.2515E 03 | 0.2802E 04 | 0.7421E-01 |
| 0.1000E 02 | 0. | 0.1185E-05 | 0. | 0.1391E-02 | 0.6918E-03 | 0.1682E-07 | 0.2090E 03 | 0.3441E 04 | 0.7396E-01 |
| 0.1200E 02 | 0. | 0.5802E-05 | 0. | 0.1146E-02 | 0.8191E-03 | 0.1441E-07 | 0.3622E 03 | 0.4046E 04 | 0.7372E-01 |
| 0.1400E 02 | 0.3370E-06 | 0.7255E-05 | 0.3368E-05 | 0.9210E-03 | 0.8937E-03 | 0.1210E-07 | 0.4140E 03 | 0.4612E 04 | 0.7349E-01 |
| 0.1600E 02 | 0.6258E-06 | 0.4002E-06 | 0.5979E-05 | 0.7246E-03 | 0.9159E-03 | 0.9994E-08 | 0.4613E 03 | 0.5138E 04 | 0.7329E-01 |
| 0.1800E 02 | 0.4083E-06 | -0.9339E-05 | 0.2764E-05 | 0.5603E-03 | 0.8938E-03 | 0.8138E-08 | 0.5050E 03 | 0.5624E 04 | 0.7313E-01 |
| 0.2000E 02 | 0.2104E-07 | -0.9823E-05 | 0.5617E-06 | 0.4273E-03 | 0.8388E-03 | 0.6554E-08 | 0.5451E 03 | 0.6071E 04 | 0.7300E-01 |
| 0.2200E 02 | 0. | 0.1143E-04 | 0. | 0.3224E-03 | 0.7633E-03 | 0.5234E-08 | 0.5819E 03 | 0.6481E 04 | 0.7289E-01 |

DESCENDING

NOZZLE HEIGHT (FT) = 0.20000000E 02

TIME = 4.0000

MOMENTUM FACTOR A = 0.74016853E-01

STAGNATION PRESSURE (PSI) = 0.50279035E-02

| STATION (FT) | DEPTH (FT) | SLOPE (DEG) | RATE (FT/SEC) | SURF. PRESS. (PSI) | DYN. PRESS. (PSI) | GAS DENS. SLUG/CU FT | PART. VEL. (FT/SEC) | GAS VEL. (FT/SEC) | TOTAL PRESS. (PSI) |
|-----------------|---------------|----------------|------------------|--------------------------|-------------------------|-------------------------|---------------------------|-------------------------|--------------------------|
| 0.1000E-04 | 0. | 0.2848E-03 | 0. | 0.5028E-02 | -0. | -0. | -0. | -0. | 0.7760E-01 |
| 0.2000E 01 | 0. | -0.9973E-04 | 0. | 0.4808E-02 | 0.2162E-03 | 0.5334E-07 | 0.7997E 02 | 0.1080E 04 | 0.7738E-01 |
| 0.4000E 01 | 0. | 0.1588E-03 | 0. | 0.4215E-02 | 0.7570E-03 | 0.4801E-07 | 0.1577E 03 | 0.2131E 04 | 0.7678E-01 |
| 0.6000E 01 | 0.1445E-04 | 0.4867E-03 | 0.4735E-04 | 0.3412E-02 | 0.1376E-02 | 0.4056E-07 | 0.2314E 03 | 0.3126E 04 | 0.7598E-01 |
| 0.8000E 01 | 0.7662E-04 | 0.5065E-03 | 0.6751E-04 | 0.2579E-02 | 0.1843E-02 | 0.3243E-07 | 0.2994E 03 | 0.4046E 04 | 0.7515E-01 |
| 0.1000E 02 | 0.4938E-04 | 0.2454E-03 | 0.6733E-04 | 0.1842E-02 | 0.2050E-02 | 0.2479E-07 | 0.3612E 03 | 0.4880E 04 | 0.7441E-01 |
| 0.1200E 02 | 0.5125E-04 | -0.5927E-04 | 0.5657E-04 | 0.1261E-02 | 0.2011E-02 | 0.1831E-07 | 0.4163E 03 | 0.5624E 04 | 0.7383E-01 |
| 0.1400E 02 | 0.4501E-04 | -0.2602E-03 | 0.4193E-04 | 0.8361E-03 | 0.1807E-02 | 0.1319E-07 | 0.4649E 03 | 0.6281E 04 | 0.7341E-01 |
| 0.1600E 02 | 0.3408E-04 | -0.2552E-03 | 0.2741E-04 | 0.5431E-03 | 0.1525E-02 | 0.9344E-08 | 0.5074E 03 | 0.6855E 04 | 0.7311E-01 |
| 0.1800E 02 | 0.2133E-04 | -0.3752E-03 | 0.1436E-04 | 0.2484E-03 | 0.1231E-02 | 0.6556E-08 | 0.5444E 03 | 0.7355E 04 | 0.7292E-01 |
| 0.2000E 02 | 0.8992E-05 | -0.2191E-03 | 0.4863E-05 | 0.2224E-03 | 0.9648E-03 | 0.4580E-08 | 0.5765E 03 | 0.7789E 04 | 0.7279E-01 |
| 0.2200E 02 | 0.9383E-08 | -0.1757E-03 | 0. | 0.1419E-03 | 0.7406E-03 | 0.3199E-08 | 0.6044E 03 | 0.8165E 04 | 0.7271E-01 |

APPENDIX B. JET TURNING ANGLE

In Appendix A, a modification to Roberts' surface loading theory was incorporated through the parameter n to account for the focusing effect of the jet when the gas expands into a nonzero pressure. If such a modification is found to be suitable when the necessary test data becomes available, it is believed that n would depend in some manner on the angle at which the jet is turned when it leaves the nozzle exit lip. During this investigation, the angle through which the jet would be turned while expanding into a perfect vacuum and a Martian environment was examined. The results of this investigation are presented here even though they had little influence on the soil erosion computations performed.

According to References 4 and 5, the jet turning angle δ is given by Figure B1 and (with a change in notation)

$$\delta = \nu_1 - \nu_e + \theta_e \quad (B1)$$

where

ν_1 = Prandtl-Meyer turning angle corresponding to the ambient stagnation pressure ratio

ν_e = Prandtl-Meyer turning angle corresponding to the nozzle exit Mach number

θ_e = nozzle exit half-cone angle

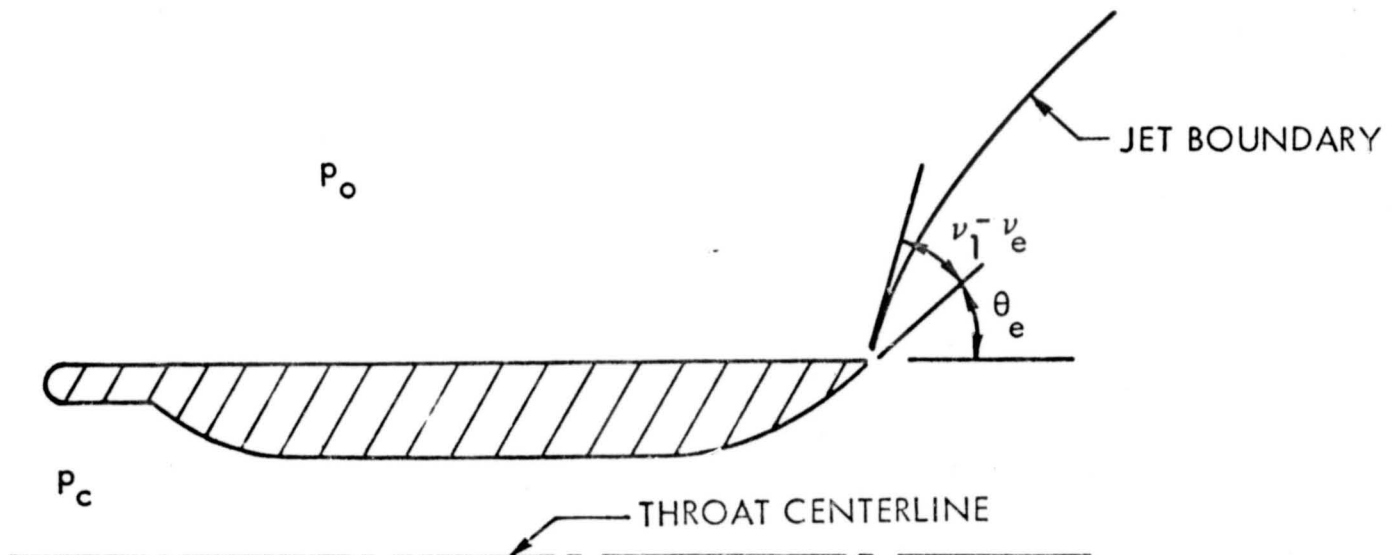


Figure B1. Jet Turning Angle Geometry

The equations given for ν_1 and ν_e are

$$\nu_1 = \sqrt{\frac{\gamma+1}{\gamma-1}} \tan^{-1} \sqrt{\frac{\gamma-1}{\gamma+1} (M_1^2 - 1)} - \tan^{-1} \sqrt{M_1^2 - 1} \quad (B2)$$

$$\nu_e = \sqrt{\frac{\gamma+1}{\gamma-1}} \tan^{-1} \sqrt{\frac{\gamma-1}{\gamma+1} (M_e^2 - 1)} - \tan^{-1} \sqrt{M_e^2 - 1} \quad (B3)$$

where

$$M_1 = \frac{2}{\gamma-1} \left[\left(\frac{p_c}{p_o} \right)^{\frac{\gamma-1}{\gamma}} - 1 \right] \quad (B4)$$

and the additional parameters are defined as

M_e = exit Mach number (dimensionless)

p_c = chamber gas pressure (psf)

p_o = ambient pressure (psf)

γ = gas specific heat ratio (dimensionless)

In a perfect vacuum ($p_o = 0$) the jet turning angle becomes

$$\nu = \frac{\pi}{2} \left[\sqrt{\frac{\gamma+1}{\gamma-1}} - 1 \right] + \theta_e \text{ (radians)} \quad (B5)$$

The solution of Equation (B5) is shown in Figure B2 for a range of gas specific heat ratios, and the solution of Equation (B1) is shown in Figure B3 for a range of ambient pressures for several specific heat ratios. For example, according to Figure B2 for a specific heat ratio of 1.252, the turning angle in a perfect vacuum would be about 114 degrees. Whereas, while expanding into a Martian ambient pressure of 0.0726 psi, the turning angle is approximately 24.6 degrees. These calculations suggest that the surface pressures under the Martian ambient pressures should be higher at the stagnation point and be confined to a smaller region on the surface than if the jet expanded into a perfect vacuum. The specific dependence of n , if one actually exists, upon these turning angles can be investigated when surface pressure test data become available.

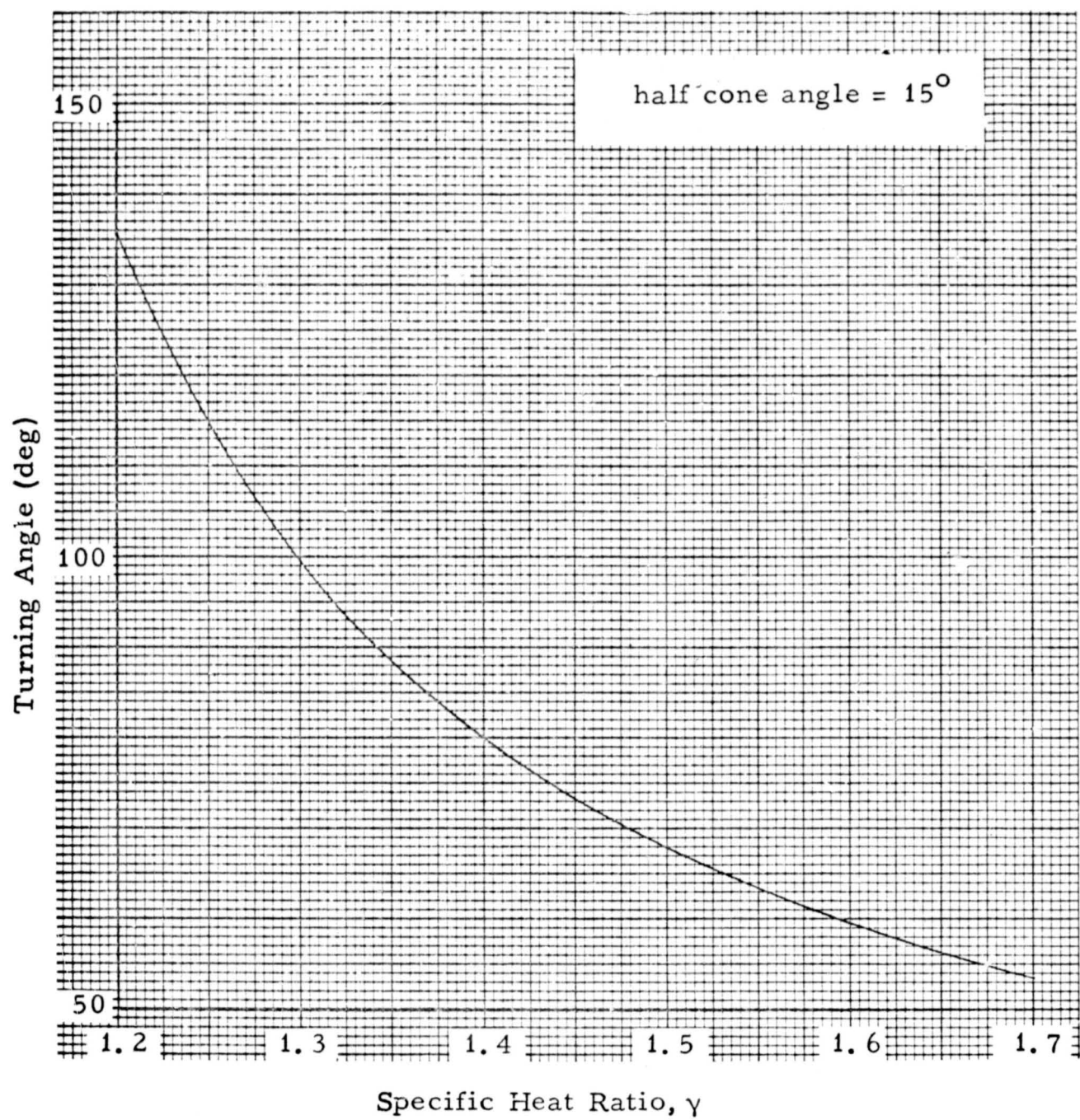


Figure B2. Variation of Turning Angle with Specific Heat Ratio-Expanding Into a Perfect Vacuum

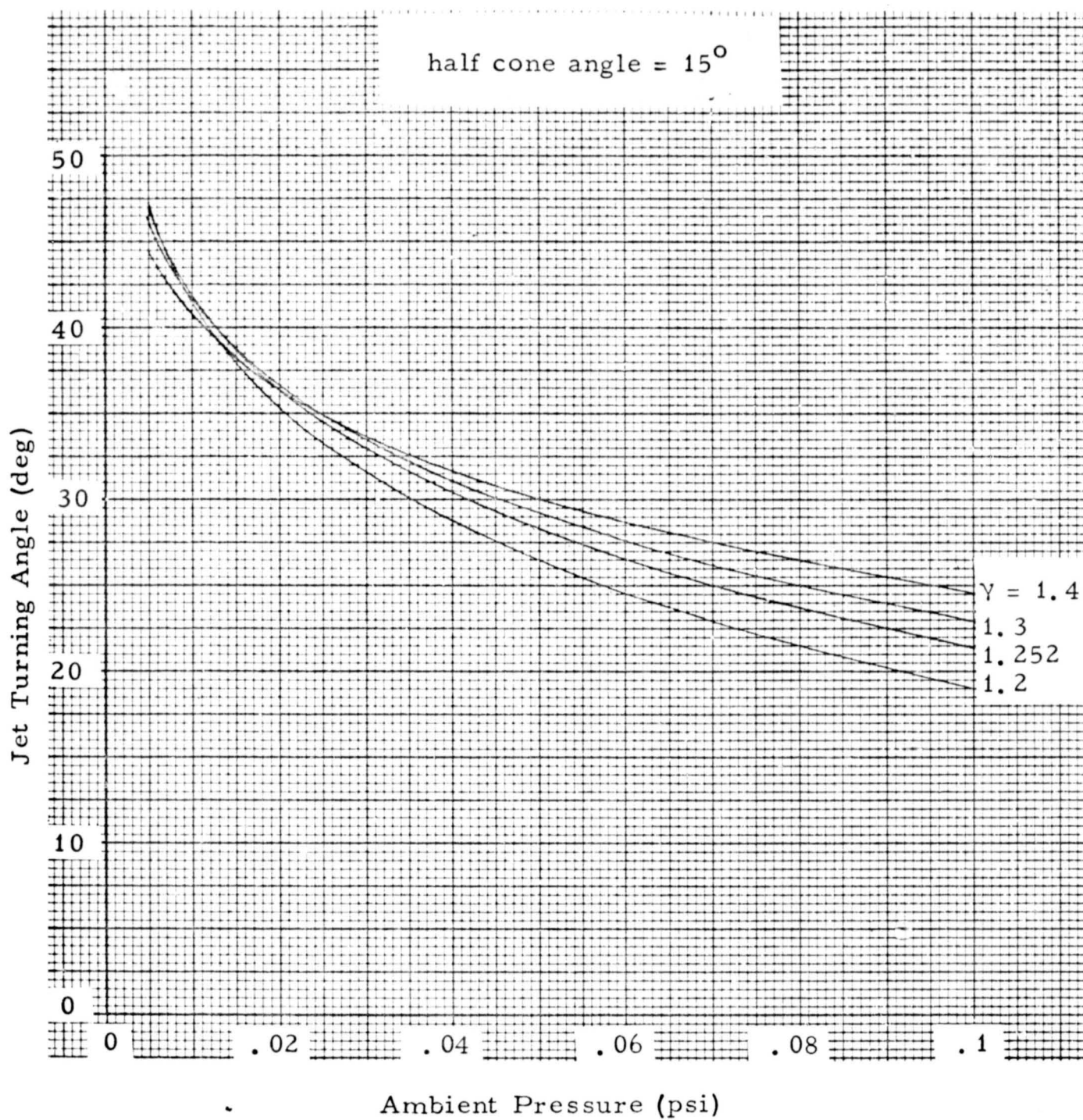


Figure B3. Variation of Jet Turning Angle With Ambient Pressure and Gas Specific Heat Ratio

APPENDIX C. PARTICLE TRAJECTORIES

This appendix considers the motion of a particle ejected from a horizontal plane surface at velocity V and angle β with the surface. After ejection the particle moves under the action of gravitational and aerodynamic drag forces. The objective of the analysis is to determine the particle impact point. The motivation for performing this analysis is because small soil particles can attain a large fraction of the gas velocity. Then, at such large velocities, their subsequent motion can be drastically altered by the presence of an atmosphere.

Figure C1 shows a typical particle trajectory. The symbols and the coordinate system used in the analysis are defined as follows:

- A = particle cross-sectional area (ft^2)
- C_D = aerodynamic drag coefficient (dimensionless)
- D = particle diameter (ft)
- K = drag parameter (ft^{-1})
- m = particle mass (slugs)
- r = particle radial displacement from point of ejection (ft)
- R = particle range in an atmosphere (ft)
- R_0 = particle range in a vacuum (ft)
- t_1 = time to reach maximum height, y_m (sec)
- t_2 = duration of flight (sec)
- u_0 = horizontal component of initial velocity = $V \cos \beta$ (ft/sec)
- v_0 = vertical component of initial velocity = $V \sin \beta$ (ft/sec)
- v_2 = vertical velocity at impact (ft/sec)
- V = particle ejection velocity (ft/sec)
- y = particle vertical displacement from point of ejection (ft)
- y_m = maximum height (ft)

β = angle at which particle leaves surface (rad)

ρ = atmosphere mass density (slugs/ft³)

σ = particle mass density (slugs/ft³)

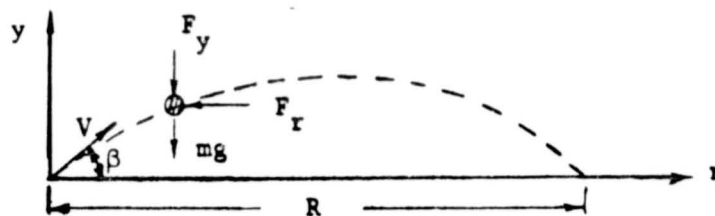


Figure C1: Typical Particle Trajectory Showing Gravity and Aerodynamic Forces

1. Particle Motion in a Vacuum

The equations of motion of a particle in the r direction in a vacuum is

$$\left. \begin{aligned} m \ddot{r} &= 0 \\ r(0) &= 0, \dot{r}(0) = u_0 = V \cos \beta \end{aligned} \right\} \quad (C1)$$

and in the y direction is

$$\left. \begin{aligned} m \ddot{y} &= -mg \\ y(0) &= 0, \dot{y}(0) = v_0 = V \sin \beta \end{aligned} \right\} \quad (C2)$$

The solution of these equations are

$$\left. \begin{aligned} r &= u_0 t \\ y &= v_0 t - \frac{1}{2} g t^2 \end{aligned} \right\} \quad (C3)$$

Eliminating time the trajectory becomes

$$y = r \tan \beta - \frac{g r^2}{2 V^2 \cos^2 \beta} \quad (C4)$$

From (C3) and (C4) one finds that

$$y_m = \text{maximum height} = \frac{1}{2} \frac{v_o^2}{g} \quad (C5)$$

$$t_1 = \text{time to reach maximum height} = \frac{v_o}{g} \quad (C6)$$

$$R_o = \text{range} = \frac{v_o^2 \sin 2\theta}{g} \quad (C7)$$

$$t_2 = \text{total flight time} = \frac{2v_o}{g} \quad (C8)$$

$$v_2 = \text{vertical velocity at impact} = -v_o \quad (C9)$$

2. Particle Motion in an Atmosphere

To account for the atmospheric drag forces one must assume a particle shape and the drag force law. It is assumed the drag force is proportional to the square of the velocity component and that the particles are spherical.

(a) Motion in r Direction

The equation of motion for the r direction is

$$m\ddot{r} = -\frac{1}{2} \rho A C_D \dot{r}^2 \quad (C10)$$

subject to the same initial conditions as the drag free case.

Now with

$$m = \frac{\pi D^3 \sigma}{6}, \quad A = \frac{\pi D^2}{4} \quad (C11)$$

one has

$$\ddot{r} = -K\dot{r}^2 \quad (C12)$$

where

$$K = \frac{3}{4} \frac{\rho C_D}{\sigma D} \quad (C13)$$

The solution of (C12) satisfying the initial conditions is

$$r = \frac{1}{K} \ln (1 + Ku_0 t) \quad (C14)$$

(b) Motion in y Direction

For motion in the y direction it is convenient to separate the total flight time into two periods; one in which the particle is ascending and the second when it is descending. During the upward motion the drag force, which opposes the velocity, acts downward, and therefore is a negative force acting on the particle. During the downward motion the drag force, which again opposes the velocity, acts upward, and therefore is a positive force acting on the particle. The initial conditions are:

$$t = 0, y = 0, \dot{y} = +v_0 \quad (C15)$$

and at the end of the ascent phase (at time $t = t_1$) the conditions are:

$$t = t_1, y = y_m, \dot{y} = 0 \quad (C16)$$

At the end of the descent phase (at time $t = t_2$) when the particle impacts the plane the conditions are:

$$t = t_2, y = 0, \dot{y} = v_2 \quad (C17)$$

Ascent Phase

The equation of motion is

$$m\ddot{y} = -\frac{1}{2} \rho A C_D \dot{y}^2 - mg$$

or

$$\ddot{y} = -K\dot{y}^2 - g \quad (C18)$$

Replacing \ddot{y} by

$$y = \dot{y} \frac{dy}{dy} = \frac{1}{2} \frac{d\dot{y}^2}{dy} \quad (C19)$$

and solving for y as a function of the velocity \dot{y} for the initial conditions given in (C15) gives

$$y = \frac{1}{2K} \ln \left(\frac{1 + \frac{Kv_o^2}{g}}{1 + \frac{Ky^2}{g}} \right) \quad (C20)$$

From (C20) the maximum upward displacement is found to be (occurs when $\dot{y} = 0$)

$$y_m = \frac{1}{2K} \ln \left(1 + K \frac{v_o^2}{g} \right) \quad (C21)$$

The velocity \dot{y} for any displacement y is

$$\dot{y} = v_o \sqrt{\left(1 + \frac{g}{Kv_o^2}\right) e^{-2Ky} - \frac{g}{Kv_o^2}} \quad (C22)$$

Upon separation of variables (C22) can be placed in the form

$$\frac{dy}{\sqrt{A^2 e^{-2Ky} - 1}} = \sqrt{\frac{g}{K}} dt \quad (C23)$$

where

$$A = \sqrt{1 + \frac{Kv_o^2}{g}} \quad (C24)$$

Integration of (C23) gives

$$\frac{1}{2} t \sqrt{gk} = \tan^{-1} \left\{ \frac{A + \sqrt{A^2 - 1} - Ae^{-Ky} - \sqrt{A^2 e^{-2Ky} - 1}}{1 + \left(A + \sqrt{A^2 - 1}\right) \left(Ae^{-Ky} + \sqrt{A^2 e^{-2Ky} - 1}\right)} \right\} \quad (C25)$$

The time $t = t_1$, when the particle reaches the maximum height corresponds to $y = y_m$. Using the definition of A given by (C24) equation (C21) becomes

$$y_m = \frac{1}{2K} \ln(A^2) = \frac{1}{K} \ln(A) \quad (C26)$$

or

$$Ky_m = \ln(A)$$

and

$$e^{-Ky_m} = \frac{1}{A}, \quad e^{-2Ky_m} = \frac{1}{A^2}$$

Using these results the time t_1 determined from (C25) becomes

$$\frac{1}{2} t_1 \sqrt{gK} = \tan^{-1} \left(\frac{A-1 + \sqrt{A^2-1}}{A+1 + \sqrt{A^2-1}} \right)$$

After a few algebraic manipulations the argument of the inverse tangent function can be written as

$$\frac{A-1 + \sqrt{A^2-1}}{A+1 + \sqrt{A^2-1}} = \frac{A-1}{B}$$

where

$$B = v_o \sqrt{\frac{K}{g}} \quad (C27)$$

and therefore the time t_1 becomes

$$t_1 = \frac{2}{\sqrt{gK}} \tan^{-1} \left(\frac{A-1}{B} \right) \quad (C28)$$

Descent Phase

The equation of motion for the descent phase is

$$m\ddot{y} = + \frac{1}{2} \rho A C_D \dot{y}^2 - mg$$

or

$$\ddot{y} = K\dot{y}^2 - g \quad (C29)$$

Proceeding along steps similar to those during the ascent phase, the first integral of (C29) is

$$- \frac{g}{K} \ln \left(1 - \frac{K\dot{y}^2}{g} \right) = - 2gy + C_1$$

where C_1 is a constant of integration. This constant is determined such that

$$y = y_m, \dot{y} = 0, t = t_1$$

and the solution becomes

$$y = \frac{1}{2K} \ln \left[A^2 \left(1 - \frac{K\dot{y}^2}{g} \right) \right] \quad (C30)$$

The impact velocity can be determined from (C30) by setting

$y = 0$ and $\dot{y} = v_2$. The result is

$$v_2 = - \sqrt{\frac{g}{K} \frac{A^2 - 1}{A^2}}$$

from which one finds that

$$v_2 = - \frac{v_0}{A} \quad (C31)$$

Returning to (C30) and solving for \dot{y} gives

$$\dot{y} = \pm \sqrt{\frac{g}{K} \frac{A^2 e^{-2Ky} - 1}{A e^{-Ky}}} \quad (C32)$$

Since y is negative during the downward motion, one takes the negative sign. Separating variables yields

$$\frac{Ae^{-Ky} dy}{\sqrt{A^2 e^{-2Ky} - 1}} = -\sqrt{\frac{g}{K}} dt \quad (C33)$$

and then integration of (C33) gives

$$-\frac{1}{AK} \cosh^{-1} (Ae^{-Ky}) = -\frac{1}{A} \sqrt{\frac{g}{K}} t + C_2$$

where C_2 is a constant of integration. This constant is determined such that at

$$t = t_1, y = y_m$$

and the solution becomes

$$t = \frac{1}{\sqrt{gK}} \left\{ \cosh^{-1} (Ae^{-Ky}) + 2 \tan^{-1} \left(\frac{A-1}{B} \right) \right\} \quad (C34)$$

The time $t = t_2$ at which the particle impacts the ground is obtained from (C34) by setting $y = 0$. Making use of the relation

$\cosh^{-1}(A) = \ln (A + \sqrt{A^2 - 1}) = \ln (A+B)$ the time t_2 becomes

$$t_2 = \frac{1}{\sqrt{gK}} \left\{ \ln (A+B) + 2 \tan^{-1} \left(\frac{A-1}{B} \right) \right\} \quad (C35)$$

The corresponding range is now obtained by substituting this value of $t = t_2$ into (C14) to obtain

$$R = \frac{1}{K} \ln (1 + Ku_0 t_2) \quad (C36)$$

One can readily verify that these solutions reduce to those obtained for t_1, y_m, t_2, v_2 and R for the drag free case, if the

series expansion (valid for small K)

$$t_2 = \frac{2v_o}{g} - \frac{7}{12} \frac{v_o^3}{g^2} K + O(K^2)$$

is introduced and the limit taken as K approaches zero.

(c) Summary

The corresponding equations listed in (C5) through (C9) obtained for the drag free case become the following for the case when aerodynamic drag is considered:

$$\left. \begin{aligned} v_m &= \frac{1}{2K} \ln (1 + Kv_o^2/g) \\ t_1 &= \frac{2}{\sqrt{gK}} \tan^{-1} \left(\frac{A-1}{B} \right) \\ R &= \frac{1}{K} \ln (1 + Ku_o t_2) \\ t_2 &= \frac{1}{\sqrt{gK}} \left\{ 2 \tan^{-1} \left(\frac{A-1}{B} \right) + \ln (A+B) \right\} \\ v_2 &= -\sqrt{\frac{g}{K} \left(\frac{A^2-1}{A^2} \right)} \end{aligned} \right\} \quad (C37)$$

where

$$\left. \begin{aligned} A &= \sqrt{1 + \frac{Kv_o^2}{g}} \quad , \quad B = v_o \sqrt{\frac{K}{g}} \\ K &= \frac{3}{4} \frac{\rho C_D}{\sigma D} \end{aligned} \right\} \quad (C38)$$

An indication of the effect of the aerodynamic drag on the range is provided by the nondimensional plot shown in Figure C2.

This figure shows the ratio of the range in atmosphere to that in a vacuum as functions of the nondimensional parameters.

$$a = \frac{Kv_o^2}{g} = \frac{3}{4} \frac{\rho C_D V^2}{\sigma D g} \cos^2 \beta$$

$$b = \frac{Ku_o^2}{g} = \frac{3}{4} \frac{\rho C_D V^2}{\sigma D g} \sin^2 \beta$$

(d) Estimate of Drag Coefficient

In an effort to estimate the drag coefficient calculations of range were made and compared with experimental data listed in Reference 6. On page 401 of Reference 6 the following data for a .30 caliber bullet are listed.

nozzle velocity = 2700 ft/sec
diameter = .308 inches
range = 500 yards, angle = 15.6 minutes (.260 deg)
range = 1000 yards, angle = 49.4 minutes (.823 deg)

Taking the air density to be 0.002378 slugs/ft³ and the density of the projectile to be 22.06 slugs/ft³ the equations derived in this appendix yielded the following results.

| Angle β (deg) | Actual Range (ft) | Theoretical Range (ft) | | |
|---------------------|-------------------|------------------------|-------------|-------------|
| | | $C_D = 0$ | $C_D = .14$ | $C_D = .15$ |
| 0.260 | 1500 | 2055 | 1462 | 1435 |
| 0.823 | 3000 | 6506 | 3060 | 2965 |

From these calculations a representative value of the drag coefficients was assumed to be $C_D = .14$.

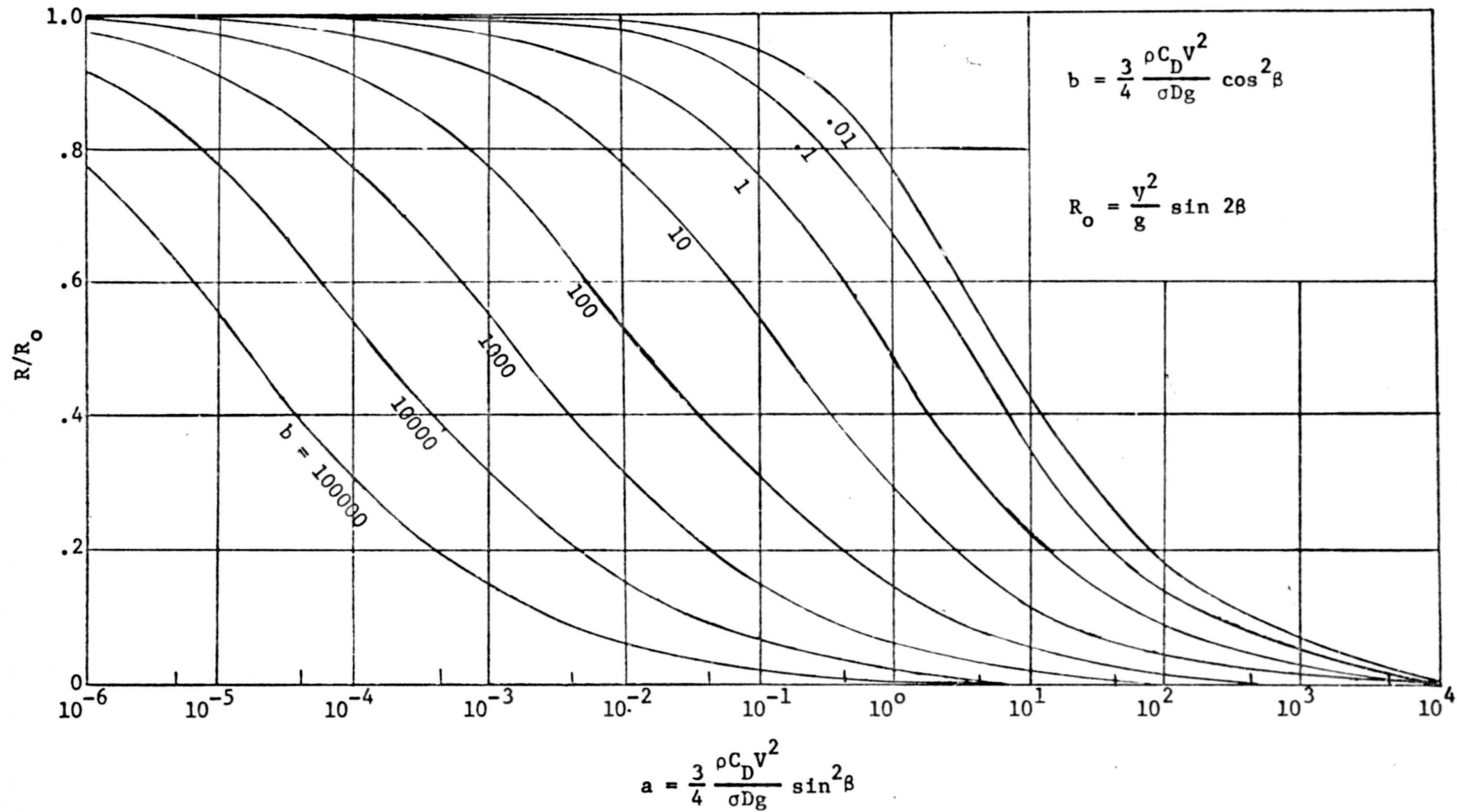


Figure C2. Particle Range Including Aerodynamic Drag